Assessment of Precast Concrete Pile Capacity using Static Load Testing and PDA Method: A Comparative Study in Kazakhstan

A thesis submitted by

Nurbek Aitzhanov

in partial fulfillment of the requirements for the degree of

Master of Science

in

Civil and Environmental Engineering

Tufts University

May 2024

Advisor: Professor Lucy C. Jen, Ph.D., PE

I. Abstract

Precast concrete piles are the common deep foundation elements utilized in Kazakhstan. This study examined the assessment of precast concrete pile capacity through Static Load Testing and Pile Dynamic Analysis (PDA) methods. For this purpose, data from two distinct construction sites in Kazakhstan were analyzed. At Site A, data revealed a close correlation between the pile capacities measured by the two methods. In contrast, Site B demonstrates significant variances in capacity results, with PDA results generally showing higher capacities than Static Load Testing. These discrepancies may be influenced by the soil heterogeneity and the limitations of the Case Pile Wave Analysis Program (CAPWAP) used to interpret field dynamic measurements, particularly in handling of soil resistance factors.

The study highlights the need for cautious application of PDA in variable geotechnical conditions and supports its integration with Static Load Testing for a more comprehensive evaluation of pile capacities in Kazakhstan's construction landscape.

II. Acknowledgments

I extend my gratitude to my advisor, Dr. Lucy Jen, for her invaluable guidance and mentorship throughout my journey at Tufts. Her feedback and direction have shaped my academic and career endeavors.

I am thankful to my committee members for their time, contributions, and comments that significantly enriched the quality of this thesis. I am grateful to Dr.Germaine for the knowledge he has shared with me throughout the journey at Tufts. Special thanks to Brian and David for their practical support and valuable advice during this journey.

My appreciation goes to Pile Dynamics Inc. for their generous support in facilitating my research with complimentary access to their extensive webinars on Pile Dynamic Analysis. This resource was crucial in deepening my understanding of the technical nuances and the interpretation of dynamic load test results.

I am profoundly grateful to the Kazakhstan Government and the Bolashak Center for International Programs for their financial support, which enabled my education at Tufts. This program plays a crucial role in cultivating professionals who will contribute to the development of the Kazakhstan Republic.

I appreciate Laura's help and support throughout my time at Tufts. She has assisted me in various aspects of my academic journey. I am also grateful to my friends Emre, George, Pad, and Cathal for shared experiences during my time at Tufts.

Lastly, but most importantly, I am grateful to my family. I am thankful to my parents for their trust and support. I owe a heartfelt thank you to my wife, Mira, for patience, and encouragement throughout this challenging yet rewarding journey. I am grateful to my children, Ansar and Alim. Their laughter, energy, and love have fueled me and made me stronger.

III. Contents

IV. List of Tables

V. List of Figures

Key Words

Precast Concrete Pile, Pile Capacity Assessment, Static Load Testing, Pile Dynamic Analysis, Kazakhstan Geotechnical Studies.

Terminology

ASTM	American Society for Testing and Materials
CAPWAP	Case Pile Wave Analysis Program
EoD	End of Driving
EMX	Mobilized Energy
FS	Factor of Safety
GOST	National Standards of the Republic of Kazakhstan
GRLWEAP	GRL Wave Equation Analysis of Piles
MLT	Maintained Load Testing
MQ	Match Quality (in CAPWAP analysis)
PDA	Pile Dynamic Analysis
PCP	Precast Concrete Pile
PLT	Pile Load Testing
QLT	Quick Load Test
RD	Restrike Dynamic Testing
Rb	Base Resistance
Rs	Shaft Resistance
Ru	Ultimate Capacity
SPT	Standard Penetration Test
Set/bl	Settlement Per Blow

Symbology

B	Diameter of the pile
Su	Pre-established ultimate average settlement
ζ	Coefficient
p	Density of pile material
u	Displacement
t	Time
E	Modulus of Elasticity of pile
Rd	Damping response of soil
F	Force
A	Area of Pile
v	Particle Velocity
Z	Impedance
Ru	Ultimate resistance of Soil
Rs	Static Resistance of Soil

1. Introduction

1.1 Problem Statement

The Republic of Kazakhstan is the ninth largest country in the world, with substantial uranium, oil, and gas reserves, positioning it as a significant player in the global energy sector (Yenikeyeff, 2008). These abundant natural resources have fueled the country's economy, notably the developments of the Kashagan oil field, with an investment of 41.2 billion USD (Oil & Gas Journal, 2013), and the Tengiz oil field Future Growth Project, with a cost of 45.2 billion USD (Oil & Gas Journal, 2019), have been at the forefront of this economic upturn. The extraction of these valuable resources necessitates the expansion of supporting infrastructure. At the same time, civic constructions has begun to be built at unprecedented rates to accommodate the growing economic activities and urbanization. As the structural loads of these constructions started to rise, there was an increasing need for deep foundation elements to support them adequately. Deep foundations are considered when structural loads must be transmitted through weak soils to deeper, more competent strata (Hussein & Likins, 1993). Kazakhstan's continental climate presents unique construction challenges, particularly during winter when temperatures fall below zero Celsius. According to Salnikov et al. (2023), data from 1971 to 2020 shows an average of 140 to 170 Frost Days (FD) annually. This environmental condition demands robust foundation solutions, and precast concrete piles have proven exceptionally resilient. Fabricated in controlled environments to ensure consistent quality and strength (Hussein & Likins, 1993), precast concrete piles have consistently maintained structural integrity despite the harsh conditions, further justifying their widespread use (Zhussupbekov et al., 2018).

However, the choice of foundation solutions varies significantly in other countries, reflecting different approaches to similar climatic challenges. Tang et al. (2023) highlight that reinforced

concrete piles of various cross-sections are used in Russia due to their durability and the material's resistance to cold weather conditions. In contrast, Canada's deep foundation elements often include steel pipe piles and H-section steel piles (Tang et al., 2023). This variation in foundation types underscores the importance of regional engineering practices and material availability, influencing the selection of the most appropriate and effective foundation solution.

Given this context, the critical issue remains to assess pile capacity for designing safe and cost-effective foundations in construction. Pile capacity is defined as the maximum load a pile can sustain without experiencing failure or excessive deformation. This concept is aligned with Vesic's (1977) definition of the ultimate load, which is identified as the load capable of causing either structural failure of the pile or failure due to the bearing capacity of the underlying soil.

Precast concrete pile capacity is assessed primarily through Static Load Testing and/or the Pile Dynamic Analysis (PDA) method (Fellenius et al., 1989). Static Load Testing, traditionally regarded as the gold standard for its accuracy (Paikowsky, 2006), entails incrementally increasing the load on a pile to observe its settlement and behavior under various loading scenarios. It simulates real-world conditions, offering a comprehensive view of the pile's performance, including its load-carrying capacity, settlement characteristics, and overall response to loading. However, it is criticized for being expensive and requiring an excessive amount of time (Paikowsky, 2006). On the other hand, the PDA method presents an alternative, offering significant advantages in terms of cost efficiency and speed (Sellountou & Roberts, 2007). The PDA method significantly diverges from static load testing by focusing on the dynamic response of a pile. This method involves observing how a pile reacts to impacts from a hammer at its top by using Pile Driving Analyzer equipment in the field. This recorded data are then analyzed using stress wave theory to estimate the resistance of the soil when the pile is under a static load,

essentially predicting pile behavior under static testing in an office setting. To refine this assessment, stress wave analysis uses a signal-matching technique utilizing the Case Pile Wave Analysis Program (CAPWAP).

The PDA method was introduced to the Kazakh Building Code in 2015 (SP RK 1.02-102-2014- stands for Collection of Regulation of the Republic of Kazakhstan). Lukpanov (2015) pioneered comparative studies of Static Load Tests and PDA methods. His research focused on the comparative analysis of four precast concrete piles, each measuring 14 meters in length and 40cm by 40cm in cross-section, used both Static Load Testing and PDA methodologies. His findings revealed a good correlation between the results obtained from both testing approaches, suggesting that the PDA could serve as a reliable alternative to static load testing under limiting settlement conditions (Lukpanov, 2015). Tulebekova et al. (2019) investigated the geotechnical challenges of the static load testing of pile capacities in Astana, revealing discrepancies when applying different standards. This emphasizes the outdated nature of Kazakhstan's static loading standards. Notably, the authors criticized the lack of modern controlling equipment, such as load cells, which are essential for accurately measuring the load applied to piles. Their work advocates for modernizing Kazakhstan's standards to incorporate such technologies. It also suggests integrating the PDA method as a complementary assessment tool alongside static load testing, highlighting its potential benefits for the industry (Tulebekova et al., 2019).

Building on the pioneering works in Kazakhstan, this study seeks to enhance our understanding of precast concrete pile capacity assessment. It delves into data from two distinct geological conditions by comparing and correlating the Pile Dynamic Analysis method with Static Load Testing. A critical aspect of this analysis involves thoroughly examining signal matching using CAPWAP. This focused approach allows us to investigate how specific factors, such as soil

parameters and the dynamics of pile installation, influence the assessed capacity of piles by the PDA method.

1.2 Thesis Objectives and Scope

1.2.1 Thesis Objectives

The objectives of this thesis are threefold:

1) To review and analyze existing literature on precast concrete pile capacity assessment methods focusing on Static Load Testing and the Pile Dynamic Analysis method. This review aims to establish a comprehensive framework for the subsequent comparative study.

2) To conduct a detailed analysis of two case studies in Kazakhstan to evaluate the effectiveness and economic efficiency (including labor, equipment, and time) of the PDA method compared to Static Load Testing in precast concrete pile capacity assessment. This analysis will provide insights into PDA's practical advantages and limitations about local geotechnical conditions.

3) To assess the potential for broader adoption of the PDA method in Kazakhstan's construction industry by considering the findings from literature and case studies.

1.2.2 Scope of the Study

This thesis's geographical and contextual focus is on Kazakhstan, specifically emphasizing current pile capacity assessment within its construction industry. The study examines precast concrete reinforced piles with lengths between 12-16 meters and cross-sectional dimensions of 300x300 mm and 400x400 mm, reflecting typical precast concrete pile specifications in Kazakhstan.

1.3 Organization of Thesis

This thesis is organized into five chapters. Chapter two will serve as the literature review, laying the foundational knowledge necessary for understanding the scope of this research. It begins with exploring deep foundation solutions, specifically precast concrete piles, discussing why this type is central to the study. The chapter defines pile capacity, elucidates its significance, and reviews the time factor influencing it. It covers Static Load Testing, followed by an examination of methods of interpretation, including comparisons between Kazakh building codes and North American practices. The PDA method and CAPWAP's roles in pile capacity assessment are then detailed, culminating in a global and local comparative analysis of both test methods.

Chapter three will present two case studies integral to this research. It details the geology, pile types, and sizes used at each site, providing context for the applied testing methods.

Chapter four outlines the research approach, detailing the tests used, the equipment employed in the investigation, and the nature and quantity of data collected. Furthermore, the chapter synthesizes the findings from the case studies, evaluating the correlation between Static Load Testing and the PDA method. This chapter aims to discern the practical implications of the research findings.

Chapter five concludes the thesis by summarizing the essential findings and offering recommendations for future geotechnical projects within Kazakhstan. It also suggests directions for further research in the field, underscoring the thesis's contribution to the geotechnical engineering discipline, particularly in Kazakhstan's construction industry.

2. Background

2.1 Deep Foundation Solutions: Focus on Precast Concrete Piles

2.1.1 Introduction to Precast Concrete Pile

Precast concrete piles are distinct from other foundation types due to their pre-manufactured nature in a controlled environment (Hussein & Likins, 1993). In Kazakhstan, this manufacturing approach ensures uniformity in construction and stringent quality control, following the standards specified in GOST 19804 (2012) (GOST stands for National Standards of Republic of Kazakhstan, which covers a range of specifications for products, services, and systems to ensure quality and safety). These piles are long, slender columns crafted from high-strength concrete with non-pretensioned steel reinforcement. Precast concrete piles are produced in various cross-sectional shapes, including square, circular, and hexagonal. However, they are mostly square, with dimensions ranging from 200x200 mm to 400x400 mm. Lengths can extend from 3000 mm to 18000 mm (Figure 2.1). The most common types of concrete piles in the USA are prestressed, primarily square, up to 750mm in cross-section (Hussein & Likins 1993).

The quality of these piles is further ensured through rigorous testing as specified by GOST 8829 (2018). Concrete strength is determined as per GOST 10180 (2012) on a series of samples made from the concrete mix. These comprehensive quality control measures ensure the reliability and performance of precast concrete piles for use in various construction projects. Seidmarova (2009) documented examples of their application in Kazakhstan, from infrastructural and residential buildings to commercial structures.

Pile Type		Width (mm)	Length (mm)
Concrete with non-pretensioned reinforcement	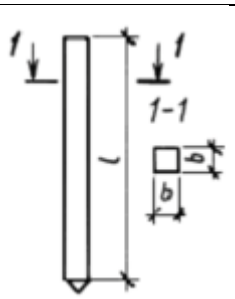	200	3000-6000
		250	4500-6000
		300	3000-12000
		350	4000-16000
		400	4000-18000

Figure 2-1 Technical specifications and dimensions of the pile with non-pre-tensioned reinforcement precast concrete piles as per GOST 19804—2012.

Transitioning to the broader context of sustainable construction, the study by Luo et al. (2019) becomes particularly relevant. Prefabricated piles have a lesser ecological impact during manufacturing and construction processes than in situ construction and can reduce greenhouse gas emissions by 11% when used (Luo et al., 2019). Thus, precast piles can have additional environmental benefits for deep foundation systems.

2.1.2 Time and Capacity of Precast Concrete Pile

Once driven, piles are tested either by the Static Load Testing or the PDA method to determine their capacity. Moreover, this test's result is assumed to represent the pile's long-term behavior and capacity (Chen et al., 1999). However, researchers found that the capacity of precast concrete piles continues to increase over time due to the phenomenon known as setup (Lee et al., 2010). This setup, or increase in bearing capacity, is observed in clay soils and is attributed to the consolidation and strengthening of the soil around the pile. Moreover, an increase in the capacity of the pile over time is observed on sandy soils. These phenomena suggest that the capacity of precast concrete piles may not be fully realized immediately after installation and that their ultimate capacity may be higher than initially measured. It is not commonly taken advantage of, resulting in significant economic loss, especially in large projects (Komurka et al., 2003).

Flaate (1972) found that the process of driving piles significantly remolds the clay around them, affecting a zone approximately 10-15 cm from the pile surface. This results in altered soil strength and deformation properties, even beyond this zone. Chen et al. (1999) found that the average unit shaft friction for a pile installed in clay, as determined from a PDA method, increased from 33 kPa to 57 kPa in 30 days post-installation. Thompson et al. (2009), reported a notable increase in shaft friction ranging between 1.8 and 3.0 times the initial end-of-drive (EoD) measurements in the clay stratum along the Biloxi Bay Area. This suggests that the bearing capacity of precast concrete piles in clay soils can significantly increase over time due to the setup phenomenon. Augustensen et al. (2005) concluded that the setup of driven piles in clay primarily involves two phases: (a) short-term effects, mainly due to the dissipation of pore pressure, and (b) long-term effects, where aging of surrounding soil plays a significant role in altering the strength and stiffness, resulting from changes in the soil skeleton and stress regime over time.

The phenomenon of setup, well-documented in clay soils, also holds significant implications for cohesionless soils such as sand. Samson and Authier (1986) discussed various case histories showing a gradual increase in pile capacity over time in sands. York et al. (1994) also examined the setup phenomena in glacial sand, noting a progressive increase in pile capacity. Furthermore, Schmertmann (1991) investigated the mechanical aging of soil, highlighting that soil aging could lead to increased stiffness, dilation, and strength, which are crucial in determining the long-term performance of precast concrete piles in sandy soils. While these studies collectively point to an increase in the ultimate capacity of precast concrete piles in cohesionless soils over time, it is essential to note that the specific mechanisms driving this increase still need to be fully understood. In certain instances, a reduction in pile capacity, known as relaxation, has been noted, as documented by Hannigan et al. (2020). Their analysis of data from 26 sites revealed that piles

installed in dense to very dense sand and shale formations are susceptible to relaxation. Consequently, they suggest overdriving piles situated in relaxation-prone zones to allow for potential future relaxation effects.

2.2 Static Load Testing

Piles are test-loaded primarily to conduct research, assess site conditions before driving production piles, and proof-test contract piles during or after installation (Fellenius, 1975). Static Load Tests are a widely recognized method for determining pile capacity (Hannigan et al., 1997). In Kazakhstan, the procedure follows GOST 5686, and internationally, ASTM D1143 provides a comprehensive framework for conducting this test. The setup for a Static Load Test involves preparing the test pile and the load application system (Figures 2-2,2-3). This setup aims to simulate the pile's field conditions as closely as possible, ensuring the test results represent the pile's performance. A reaction system using kentledge (dead load) or reaction piles is established to provide the necessary resistance for load application (Whitaker & Cooke,1961). Kentledge refers to a system of dead weights used to test piles, which can be made of concrete blocks or other heavy materials (Figure 2-2). Load is applied by using a hydraulic jack, and reaction piles are used as a counterforce in load testing (Figure 2-3). They are driven into the ground near the test pile and connected through a beam or frame over the test pile. When load is applied to the test pile, the reaction piles provide the necessary resistance (Figure 2-3). Displacement gages and load cells are used to capture the pile's response to the applied loads accurately. Using the data collected from the displacement gages and load cells, a plot of the relationship between the applied load and the pile head's resulting settlement is constructed. By analyzing the load-settlement curve (Figure 2-4), engineers can evaluate the pile's behavior under different loading conditions and gain insights into its performance characteristics. Additional Description of Figure 2-4: (a) Friction pile in soft-

firm clay or loose sand (b) Friction pile in stiff clay (c) Pile bearing on weak porous rock (d) Pile lifted off seating on a hard rock due to soil heave and pushed down by test load to new bearing on rock (e) Gap in pile shaft closed by test load (f) Weak concrete in pile shaft sheared completely through by test load.

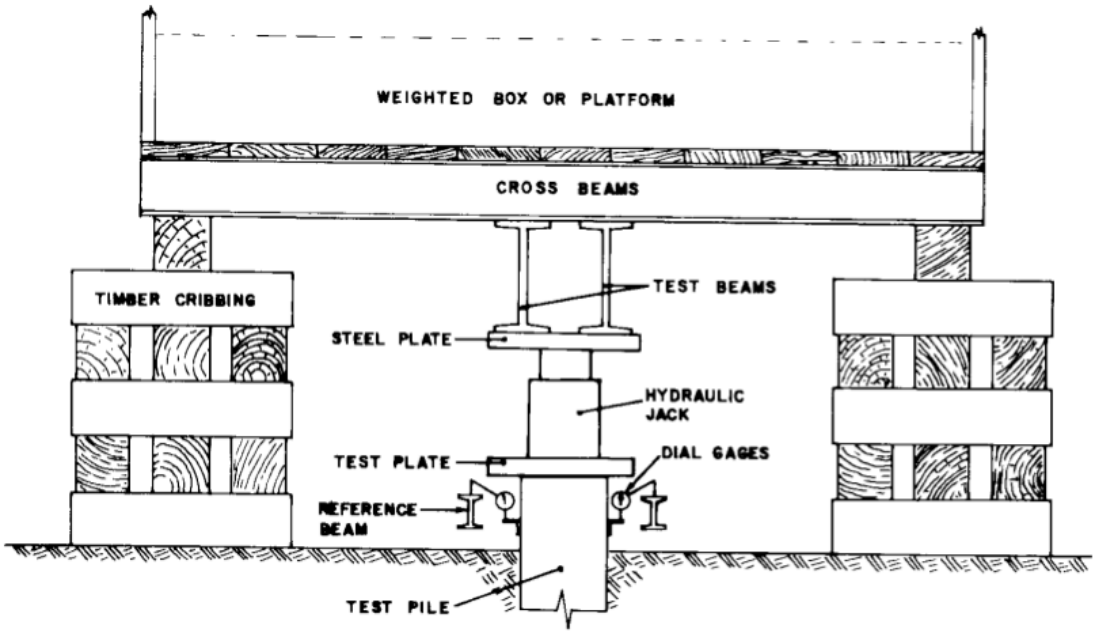

Figure 2-2 Schematic Setup for applying loads to the test pile using a hydraulic jack acting against the reaction platform. Adopted from ASTM D1143-1994.

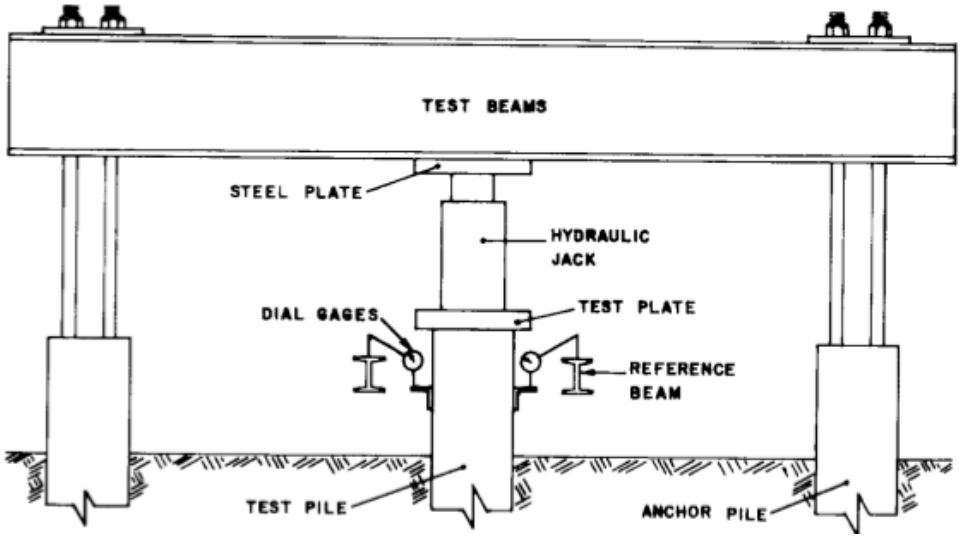

Figure 2-3 Schematic Setup for applying loads to pile using hydraulic jack acting against anchored reaction frame. Adopted from ASTM D1143-1994

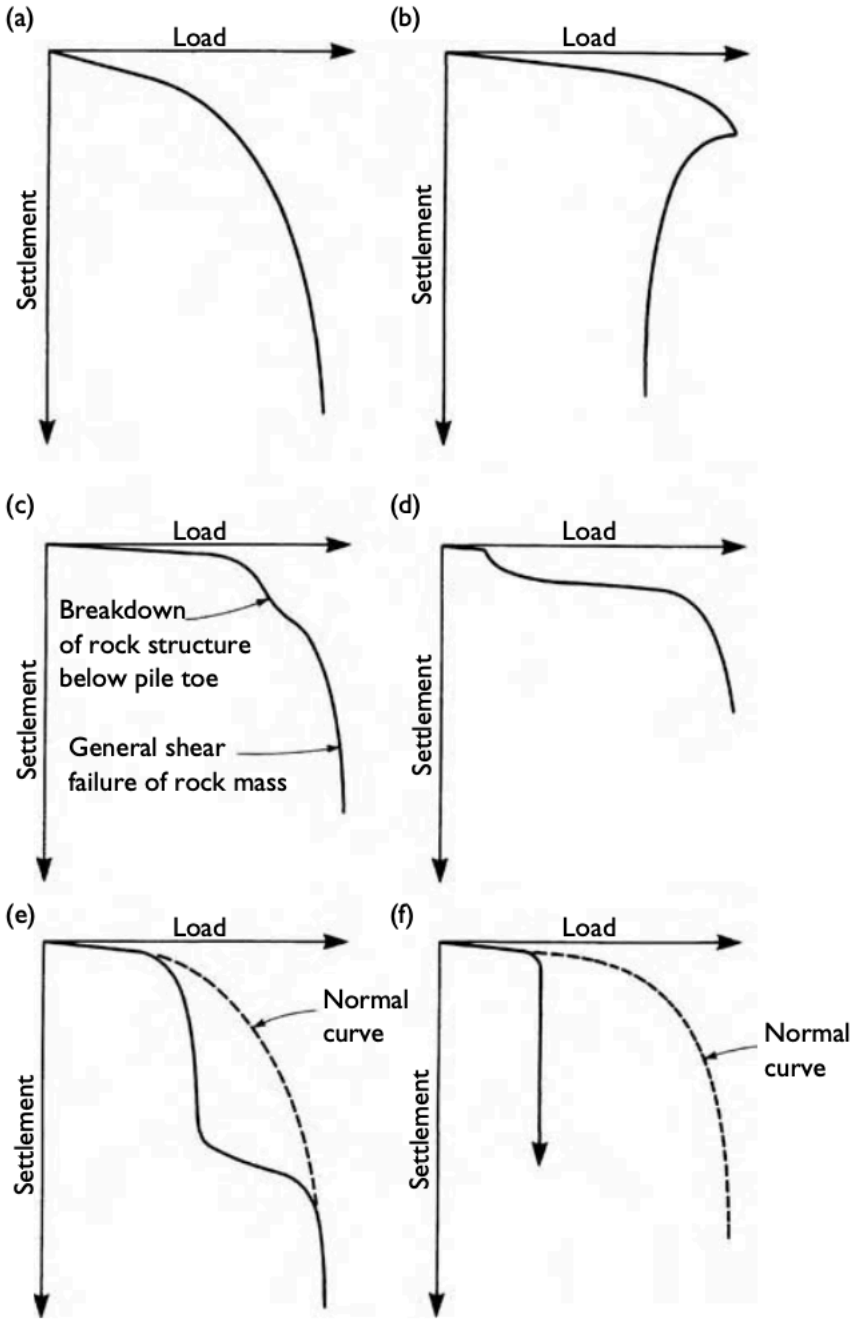

Figure 2-4 Typical load-settlement curves for compressive load tests. Adapted from Tomlinson and Woodward (2008, p. 530).

However, the effectiveness of these tests is contingent on the accuracy of the equipment used. This brings us to the analysis provided by Tulebekova (2015), who critiqued the GOST 5686-94 standard for its lack of updates since 1994 and contrasted it with the continuously updated ASTM

D1143, incorporating the latest technological advancements. She pointed out the omission of load cells as essential equipment for controlling the applied load during testing. However, it is important to note that the GOST standard has since been updated in 2020, incorporating modern technological advancements to align more closely with current engineering practices. This update addresses previous criticisms, including containing load cells for accurate measurement. This enhancement aligns with Fellenius's (1984) emphasis on the importance of employing monometers and load cells to measure the applied load accurately. Fellenius found that without such measures, the error margin in loading could reach approximately 15 percent, underscoring the potential discrepancies and inaccuracies arising from adhering to outdated standards.

Furthermore, the main distinction between the ASTM D1143 and GOST 5686 standards lies in their requirements for the pile's stabilization rate before proceeding to the next loading step. ASTM mandates a stabilization rate of 0.25mm/hr, contrasting with GOST's more stringent requirement of 0.1mm/hr. This difference is crucial as it can significantly impact the overall results and analysis of the pile test, suggesting that even with the technological updates in GOST, operational differences in testing protocols remain.

Additionally, Lukponov's work (2016) provides a detailed analysis for an in-depth comparison of both methods, highlighting the procedural and outcome differences between the ASTM D1143 and GOST 5686 standards.

Table 2-1 Static Load Testing in accordance to GOST 5686 and ASTM D 1143

Parameters	GOST 5686	ASTM D1143
Load Increments	0.1-0.1 of maximum test load	MLT, CLT % of desing, QLT 10-15% of design
Time interval for removal of recordings of intermediate load steps based on deflectometers	Every 15 min over course of first hour of observation, every 30 min over coarse of second hour, and every 60 min thereafter to conditional stabilization	MLT, CLT. After load application, then every 10 min over course of first 30 min, and every 20 min thereafter.
Unload increment	Steps equal to twice load step	MLT: In same sequence as loading. CLT: At steps equal to twice values of load steps. QLT. Total surcharge.
Conditional-stabilization criterion	Settlement of 0.1 mm after 60min	Settlement of 0.25 m after 1 h of observation
Distance from test pile to supports of reference system	no less than 2 m	No less than 2.5 m

2.3 Interpretation of Static Load Test Results

The information obtained from the static load test enables determining a pile's capacity based on a specified failure criterion (Fellenius 1980). A pile's capacity is defined as the load at which pile movement increases disproportionately to the load (Likins et al., 2011). Since then, numerous methods for interpreting test results have been introduced to address challenges, including load-test curves lacking a clear failure load and instances where some piles may not reach ultimate capacity. This development was driven by the need to understand and define failure criteria for ultimate pile capacity, given the limitations observed in traditional testing approaches (Goble et al., 2000).

Davisson's (1972) offset limit criteria (Figure 2-5), as highlighted by Fellenius (1980), was found to be the best approach to evaluate the test results of driven piles. Likins and Rausche (2004), advised that to correlate better the CAPWAP and Static test results, the load-settlement curve should be interpreted by the Davisson criteria. Therefore, this study will analyze this method of interpretation alongside with the local Kazakh building code.

The Davisson Offset Limit is articulated as the load that prompts a displacement exceeding the pile's elastic compression and is defined in Equation 2.1, Where X (in mm) is the offset displacement of the elastic compression line, and B is the diameter of the pile in mm (for the square pile width is taken as the diameter). This Offset Limit Load, as defined, does not necessarily denote the pile's ultimate resistance but approximates a perceived capacity at a minimal toe movement, adjusting for the pile's stiffness based on its material, length, and diameter, as detailed in the "Basics of Foundation Design" (Fellenius, March 2023).

$$X = 3.8 + \frac{B}{120} \qquad \textit{Eq 2.1}$$

Where X (in mm) is the offset displacement of the elastic compression line, and B is the diameter of the pile in mm.

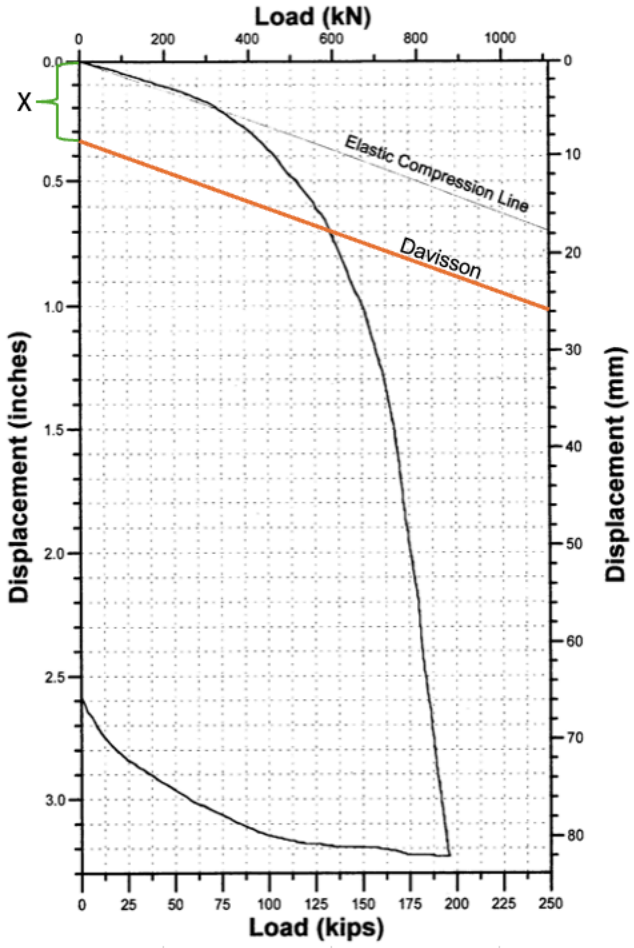

Figure 2-5 Load-Settlement Curve of Pile. Adopted from Paikowsky et al., 1994.

In the context of the Kazakh building code Construction Norms and Regulations of Pile Foundations of the Republic of Kazakhstan (SNiP RK 5.01-03-2002), the ultimate capacity of a pile during static load testing is determined by distinct failure criteria. Specifically, if the static load applied to the pile causes it to displace 20mm or more, this displacement is accepted as the pile having reached its ultimate capacity. However, in scenarios where this level of displacement is not observed, an alternative calculation is employed. This involves measuring the load that causes the pile to settle to a depth 'S', which is not arbitrary but calculated according to a precise formula:

$$S = \zeta * Su \qquad Eq\ 2.2$$

Where Su represents the pre-established ultimate average settlement value for the building or structure's foundation, as stipulated by the SNiP RK 5.01-01-2002 standard (Table 2.1), the coefficient ζ, is set to 0.2, aligning with the conditions where the pile testing adheres to a conditional settlement stabilization rate of 0.1 mm per hour.

LIMITING FOUNDATION DEFORMATIONS	
Structures	Average Su, in [brackets maximum Su(max),] settlement, cm
1. Industrial and civil single-storey and multi-storey buildings with a full frame:	
Reinforced concrete	[8]
Steel	[12]
2. Buildings and structures in the designs of which no forces from non-uniform settlements occur	[15]
3. Multi-storey frameless buildings with load-bearing walls made of:	
Large panels	10
Large blocks or brickwork without reinforcement	10
The same, with reinforcement, including the arrangement of reinforced concrete belts	15

Figure 2-6 Limiting Foundation Deformation as per SNiP RK 5.01-01-2002

2.4 Pile Dynamic Analysis by Wave Equation

Pile Dynamic Analysis testing is a pivotal technique that evaluates pile behavior and integrity under simulated service loads. This method, predicated on the analysis of stress waves generated by striking the pile top with a hammer, offers insights into the pile's capacity, resistance distribution, and potential structural issues. In Kazakhstan, this method adheres to GOST 5686 and globally to ASTM D4945-12 standards and codes, delineating the procedures and specifications for conducting dynamic load tests on deep foundations. The exploration of this testing technique with wave equation analysis and interpretation by CAPWAP in the following sections are deeply informed by the extensive resources provided by Pile Dynamics Inc.

2.4.1 Wave Equation Analysis of Piles-WEAP

It has been known since the 1930s that pile driving must be analyzed by employing the theory of wave propagation, as discussed by Fellenius (2023, pg 9-12). In the 1950s, E.A. Smith (1960) embarked on a pioneering investigation into wave propagation phenomena in slender rods (piles), laying the groundwork for what would become a cornerstone of modern geotechnical engineering practice. This equation is represented as follows:

$$\rho\frac{d^2u}{dt^2} = E\frac{d^2u}{d^2x} \pm R_d \qquad \textit{Eq 2.3}$$

Where: ρ=density of pile material, u=displacement, t=time, E=modulus of elasticity of pile, R_d=damping response of soil, $\frac{d^2u}{dt^2}$= the acceleration of a particle in the pile with respect to time, $\frac{d^2u}{d^2x}$ =displacement of a particle in the pile with respect to position.

This numerical analysis method, a significant advancement at the time, was designed to predict the relationship between pile capacity and blow count. Smith's approach (1960) utilized a one-dimensional mathematical model that represented the hammer and its components—including the ram, cap, and cap block—as well as the pile itself as a series of lumped masses and springs (Figure 2.7). Smith's revolutionary model provided engineers with a tool to assess pile behavior under hammer impacts quantitatively.

Building upon Smith's foundational work and the advancements in dynamic monitoring, GRLWEAP (GRL is the company name, Wave Equation Analysis of Pile) emerged as a sophisticated simulation tool designed to optimize pile-driving operations (Goble & Rausche, 1976). GRLWEAP extends the principles laid out by Smith, incorporating advanced computational techniques to simulate the interactions between the pile, hammer, and soil during the design stage of the foundational project. This software enables engineers to predict the behavior of pile

foundations under various driving conditions, facilitating the selection of appropriate hammers and driving strategies to ensure efficient and safe pile installation. Throughout its development, the GRLWEAP program, its hammer models, hammer data, and driving system files have undergone various updates.

Parallel to the advancements in pre-driving analysis facilitated by the GRLWEAP, the development of the CAPWAP represented a significant milestone in post-driving evaluation (Goble et al.,1972). CAPWAP, leveraging the principles of wave equation analysis, processes data from field measurements to assess the actual performance of piles after installation. By comparing measured force and velocity with those predicted by the wave equation model, CAPWAP refines the soil resistance parameters, offering a detailed evaluation of pile capacity and integrity.

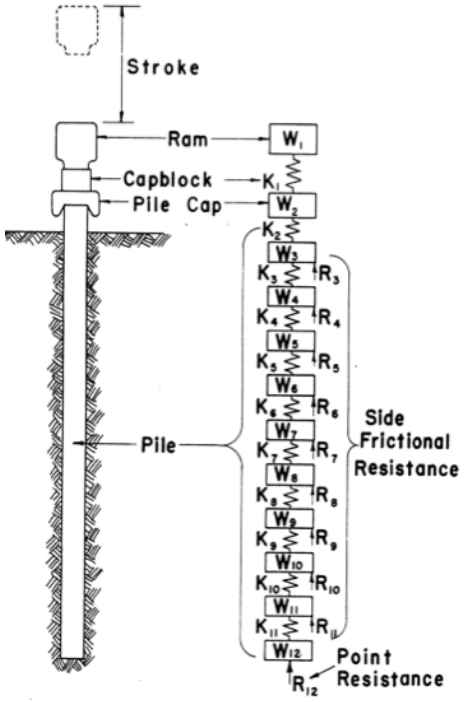

Figure 2-7 Pile-Soil Model for Smith's analysis (Adopted from Smith,1960)

2.4.2 GRLWEAP Overview

GRLWEAP's effectiveness is underpinned by its detailed models, which simulate the behavior of the pile, hammer, soil, and drive system during the driving process. Each model plays a crucial role in ensuring the accuracy of the simulations.

Pile Model: GRLWEAP's pile model encompasses various pile types, including concrete, steel, and timber, accounting for their unique properties and behaviors. The model considers the pile's length, cross-sectional area, material properties, and the interaction between the pile and the soil. It simulates the pile as a slender elastic rod, enabling the calculation of displacements along its length during driving.

Hammer Model: The hammer model in GRLWEAP simulates different types of hammers, including drop hammers, diesel hammers, and hydraulic hammers. It accounts for the hammer's mass, impact velocity, and energy transfer efficiency. The model also considers the effect of cap block materials and the hammer's operating conditions on the stress waves generated during impact.

Soil Model: GRLWEAP's advanced soil model, which incorporates parameters such as soil resistance, damping, and quake, is at the heart of its simulation capabilities. The soil resistance factor plays a pivotal role in simulating the interaction between the pile and the soil, impacting the pile's capacity and the stresses induced during driving. Damping parameters address the energy dissipation as the pile moves through the soil, while the quake value represents the threshold of soil deformation at which maximum static resistance is mobilized.

Drive System Model: This model simulates the interaction between the ram, cap block, and pile cap, integral components of the drive system. It considers the effects of these components on the

efficiency of energy transfer from the hammer to the pile and the resulting stress distribution along the pile during driving.

GRLWEAP provides several analysis options, enabling engineers to tailor their simulations to specific project requirements. These options include:

Bearing Graph Analysis: This analysis aids in the selection of pile-driving equipment by predicting the capacity of piles at varying energy levels. It ensures that the selected hammer is appropriately sized to drive the pile to its required capacity without causing undue stress (Figure 2-8).

Inspectors' Chart: The Inspectors' Chart function offers a real-time validation tool for assessing achieved pile capacities during construction. It provides predictions of required blow counts for different hammer strokes, ensuring that the piles meet design specifications (Figure 2-9).

Drivability Analysis: This option integrates static and dynamic soil resistance models to forecast the required blow counts for achieving specified depths. Drivability Analysis offers invaluable insights into potential driving issues, enabling engineers to anticipate and address challenges before they arise.

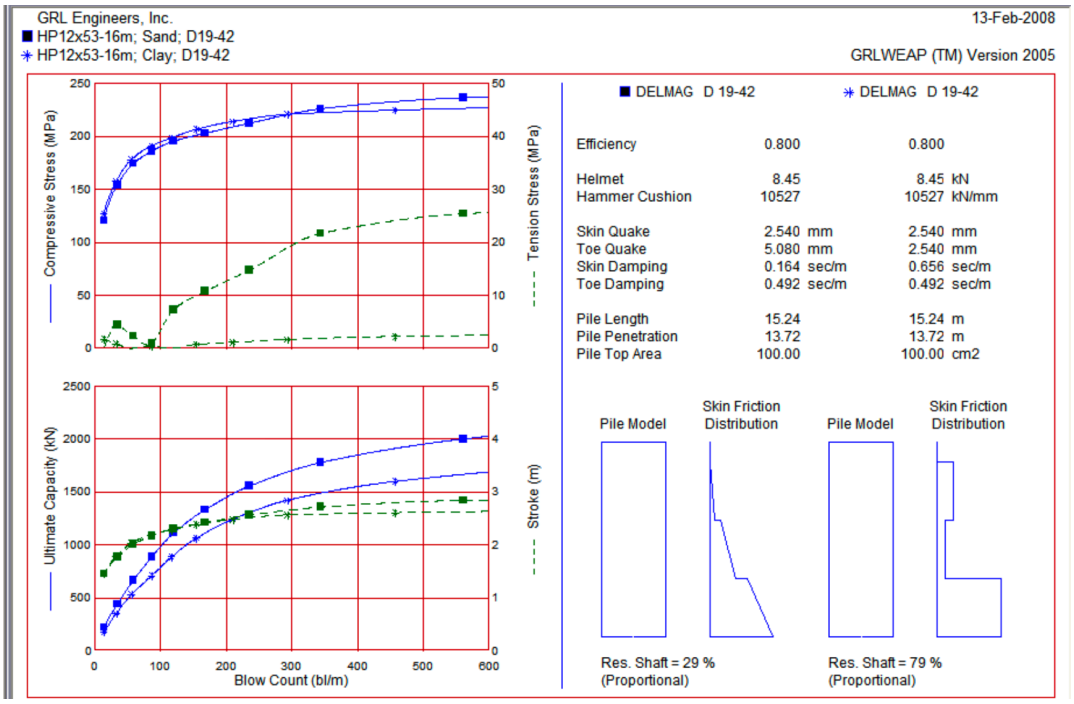

Figure 2-8 Bearing Graph Example. Adopted from Pile Dynamics

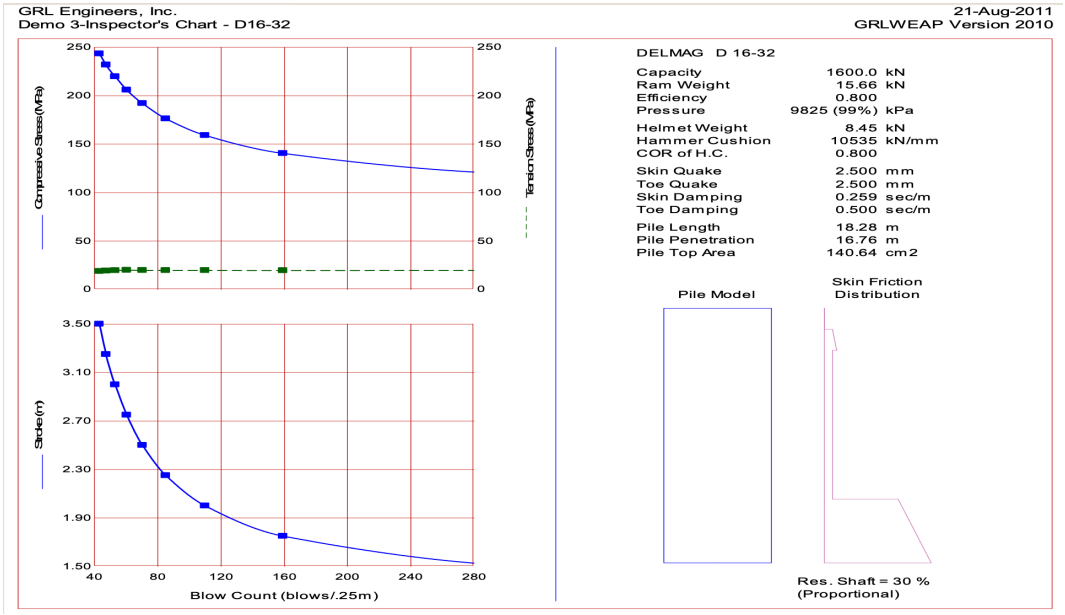

Figure 2-9 Inspectors Chart Example. Adopted from Pile Dynamics

2.4.3 Pile Driving Analyzer and Interpretation by Case Pile Wave Analysis Program

The true potential of wave equation analysis was unlocked when it was integrated with dynamic monitoring techniques during pile driving, a concept pioneered in the early 1970s by researchers at Case Western University (Goble et al., 1975). This dynamic monitoring involves recording and analyzing strain and acceleration within the pile triggered by the impact of the hammer (Figure 2-10).

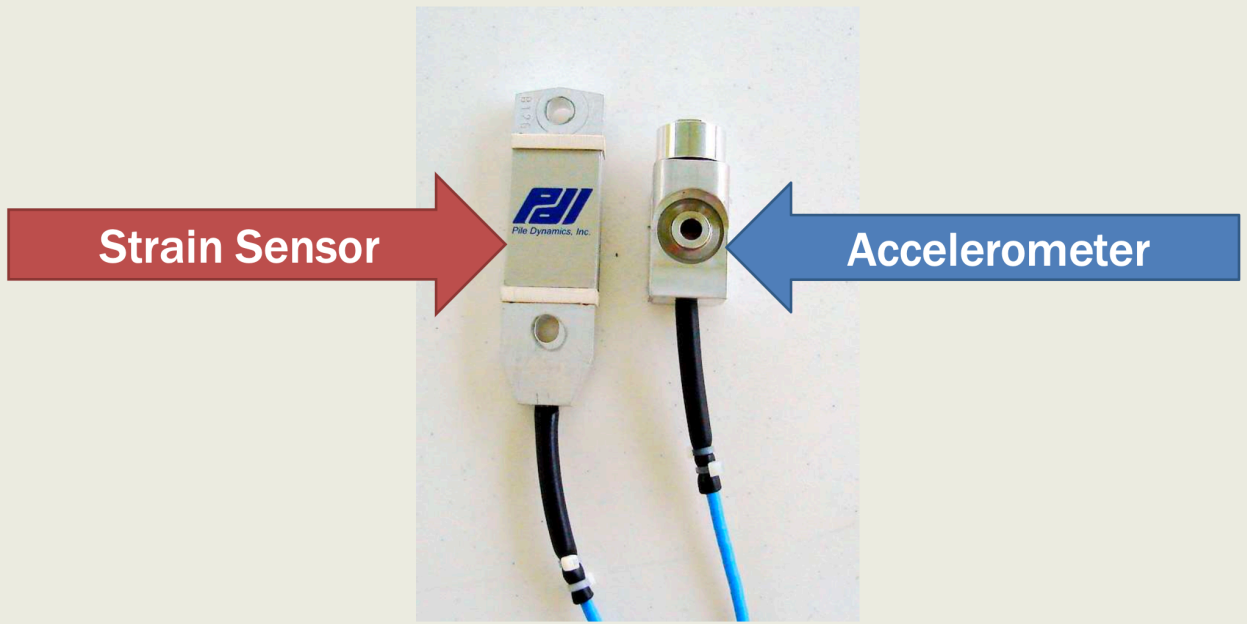

Figure 2-10 Force and Velocity Measurement sensors. Adopted from Pile Dynamic

When a hammer strikes the pile head, a compressive stress wave travels down the pile at a speed c, which is a function of the pile elastic modulus E and mass density. The impact at the pile head induces a force F and a particle velocity v in the pile.

$$F = v * \left[E * \frac{A}{c}\right] = v * Z \qquad \textit{Eq 2.4}$$

Where A is the cross-sectional area of the pile, and $E * A/c$ is the impedance and is referred to as Z. If the pile is uniform and infinitely long and there is no soil resistance, then the measured force and measured velocity multiplied with pile impedance (Z) are the same. As a result of soil

resistance, part of the down-traveling wave is reflected at the pile tip and separates the measured force and measured velocity (Figure 2-11). The magnitude of the reflected wave is proportional to the dynamic resistance of the soil. So, it is possible to determine the down-traveling wave and the up-traveling wave generated by the soil static resistance by equation 2.5, where cap R_u is ultimate resistance, cap R_d is soil dynamic resistance, and R_s soil static resistance.

$$R_u = R_d + R_s \qquad \textit{Eq 2.5}$$

For precast concrete piles, a pair of accelerometers and a pair of strain transducers are attached at least two pile diameters below the pile head, maintaining that sensors are above the waterline or ground level (Figure 2-11). Sensors are connected to the Pile Driving Analyzer that internally performs all the necessary signal conditioning and processing to obtain output results during driving for each hammer blow and immediate screen display of measured force at the pile head ($F_{measured}(t)$) and pile head movement velocity ($v_{measured}(t)$) as a function of time (Figure 2-11). Also, down and up traveling waves in a pile could be displayed in real-time for each blow. All data are recorded so it can be re-analyzed. The method and procedure of measurement is standardized globally by the standard ASTM D4945, and locally by the standard GOST 5686.

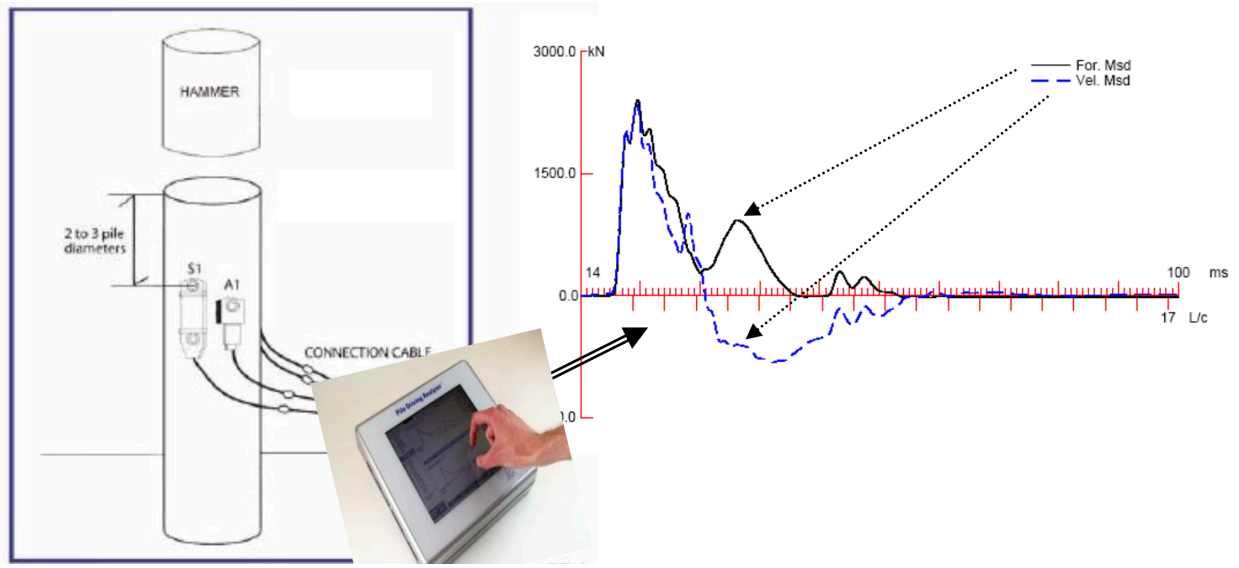

Figure 2-11 Force and Velocity measurement by Pile Driving Analyzer. Adopted from Pile Dynamics

After the execution of the field part of the PDA, recorded blow data are analyzed in the CAPWAP program. This process is outlined in Figure 2-12. The pile and soil models are initiated with measured values of pile velocity and force (Figure 2-13). The result of CAPWAP analysis is a calculated response of force, which should be completely identical to the measured one in the case of perfectly accurate pile and soil model data.

However, since the pile model is known but the soil model is unknown, there is always a difference between $(F_{calculated}(t))$ and $(F_{measured}(t))$. The soil model parameters for each pile segment that interacts with the ground are adjusted until no further improvements can be made in the match quality between the calculated and measured force signals. The maximum activated pile toe displacement and static capacity of the tested pile can be calculated with a satisfactory approximation of forces and soil model properties. A pile load-displacement graph and summary results table are obtained with progressive loading of the defined pile-soil model (Figure 2-14).

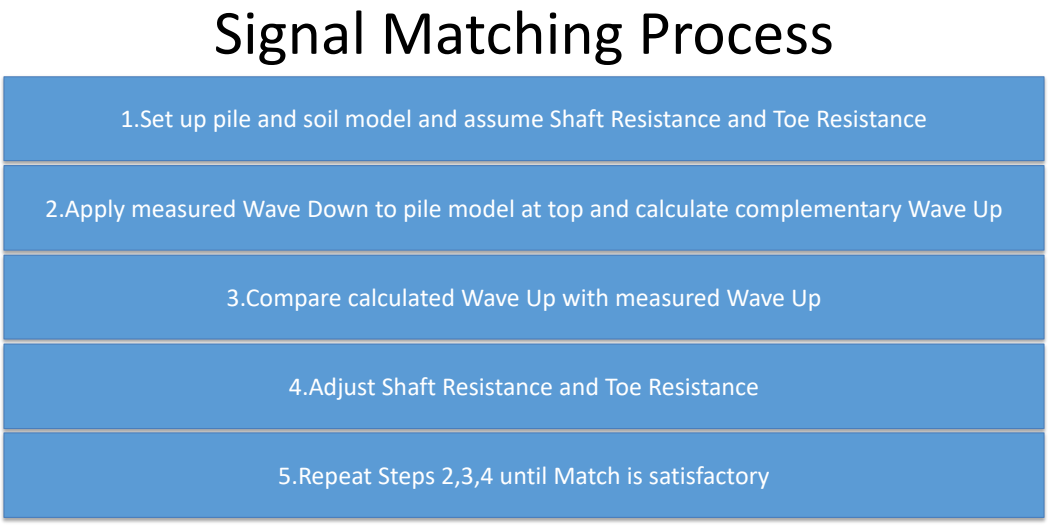

Figure 2-12 The signal matching flow chart of CAPWAP Analysis

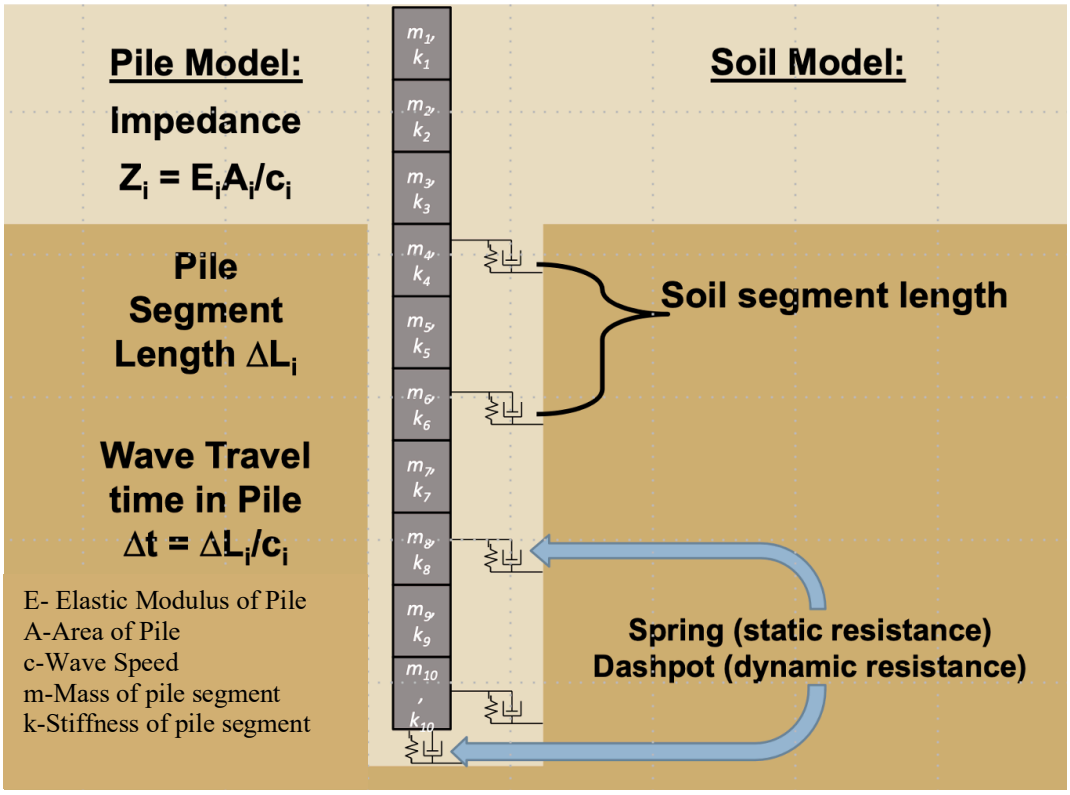

Figure 2-13 Pile-Soil Model in CAPWAP

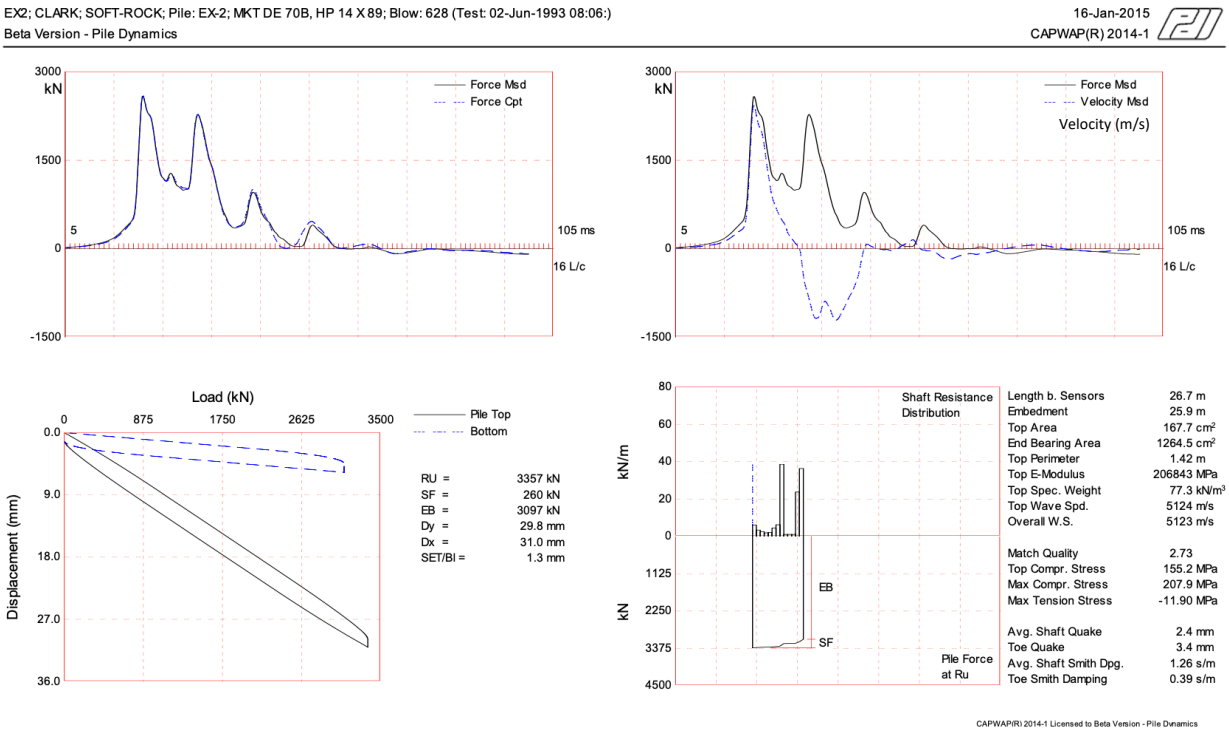

Figure 2-14 Load-Displacement Graph obtained by CAPWAP. Adopted from Pile Dynamics.

Where RU is Ultimate resistance, SF is shaft resistance, EB is base resistance, Dy is average pile head movement, and Dmx is the maximum pile head movement. Match Quality is the indicator of how the measured and computed forces match. Match qualities of 5 and less are good estimates of mobilized pile capacity, and values greater than 5 shall be evaluated conservatively.

2.4.4 Limitations of Pile Dynamic Analysis Method

The effectiveness of Pile Dynamic Analysis method for evaluating pile capacities is not without its limitations. One significant limitation is the dependency on the driving hammer's mass and drop height to generate enough energy to activate the foundation's resistance for proper capacity evaluation. Additionally, the strategic placement of measurement devices is crucial; they must be situated sufficiently above the ground and distant from the pile head, a requirement that typically leads to the excavation around the pile, adding complexity to the process.

Paikowsky (2006) highlights a specific restriction related to the soil model enhancements: the scant information obtainable from the dynamic responses at a singular measurement point limits the potential for model refinement. This constraint on available data narrows the scope for improving the soil model. Moreover, Svinkin (2002) casts doubts on the process of signal matching used in PDA by questioning the existence and definiteness of the "optimal approximation" for a measured curve. He points to the relationship between the quantification of pile capacity and the match quality indicator as a sign of the intrinsic uncertainties present in the signal-matching determination of pile capacities.

2.5 Correlation of Static Load Testing and Pile Dynamic Analysis Method

Many researchers have studied the correlation between the results obtained from the pile dynamic analysis method and static load testing to evaluate the former's reliability and accuracy in predicting pile capacity.

Likins and Rausche's (2004) analysis of 303 cases found a good correlation between CAPWAP restrike outcomes and static load test results, particularly when comparing both tests that were performed after similar waiting times. Their research articulated that discrepancies between CAPWAP and static load test data are generally within the expected variance of Static Load Test failure loads determined by multiple evaluation methods. Such parallels were found by Fellenius et al. (1989) who discerned a notable concordance between CAPWAP findings and Static Load Test results in their exploration of driven piles. Further, R. E. Lukpanov's (2015) study conducted in Western Kazakhstan on precast concrete pile capacities advocated that comparable outcomes are achievable when limiting-allowable settlement criteria is used to evaluate load settlement curves.

Diverging slightly, Svinkin's (2002) study analyzed 39 piles, which underwent both PDA and Static Load Testing. Although a comparable match was observed for 27 piles within the acceptable error margins, 12 piles displayed less precise capacity calculations. This highlights that while the pile dynamic analysis method can often align with static load testing, the congruence is not uniformly guaranteed.

Aoki and de Mello's 1992 study of energy effects in CAPWAP results revealed that pile capacity could be mobilized at varied energy levels, suggesting that energy mobilization, while necessary, is not the sole determinant of pile capacity. This study also challenged the conventional wisdom that damping and quake parameters in the Smith model are constant, demonstrating their dependence on the energy level, hence advocating for a nuanced approach beyond single blow-and-set data.

As stressed by Fellenius (1988), proficiency in CAPWAP analysis is not achieved overnight. To underscore the complexity and skill required, he states: "While the principles involved are simple, the analysis necessitates education in aspects of soil mechanics and in the practice of piling installation. The iterative procedure employed requires frequent judgment decisions. Therefore, not until after many and long hours of training is the CAPWAP engineer able to perform commercially viable analyses." Complementing this perspective, Svinkin (2004) stated that, despite the Pile Dynamic Analysis method having robust support from both hardware and software, it evidently lacks an engineering foundation.

Fellenius (2023) states that the cost of one conventional static test equals the cost of ten to twenty pile dynamic analyses, sometimes more. In the same work, he states that: “pile capacity can vary considerably from one pile to the next, and the single pile chosen for a static loading test may not be fully representative for the other piles at the site. The low cost of the dynamic test means that

for relatively little money, when using pile dynamic analysis, the capacity of several piles can be determined. Establishing the capacity of several piles gives greater confidence in the adequacy of the pile foundation, as opposed to determining it for only one pile. Therefore, the PDA/CAPWAP applied to a driven pile project ensures a greater assurance for the job".

3. Site A and Site B Introduction

3.1 Geotechnical Profile of Site A

Site A has been selected as the location for a civic multistory building. The cross-section of the area is detailed in Figure 3-1. Based on an extensive subsoil investigation conducted by an independent third party, the soils within the study area have been classified into distinct layers, arranged in the stratigraphic sequence of their occurrence. The geotechnical survey provided a comprehensive understanding of the subsurface conditions, enabling the identification and characterization of the soil strata. This detailed stratification is crucial for the geotechnical analysis and design of the foundation system for the proposed development at the site. Each of these layers are described to provide a thorough understanding of the site's geotechnical properties.

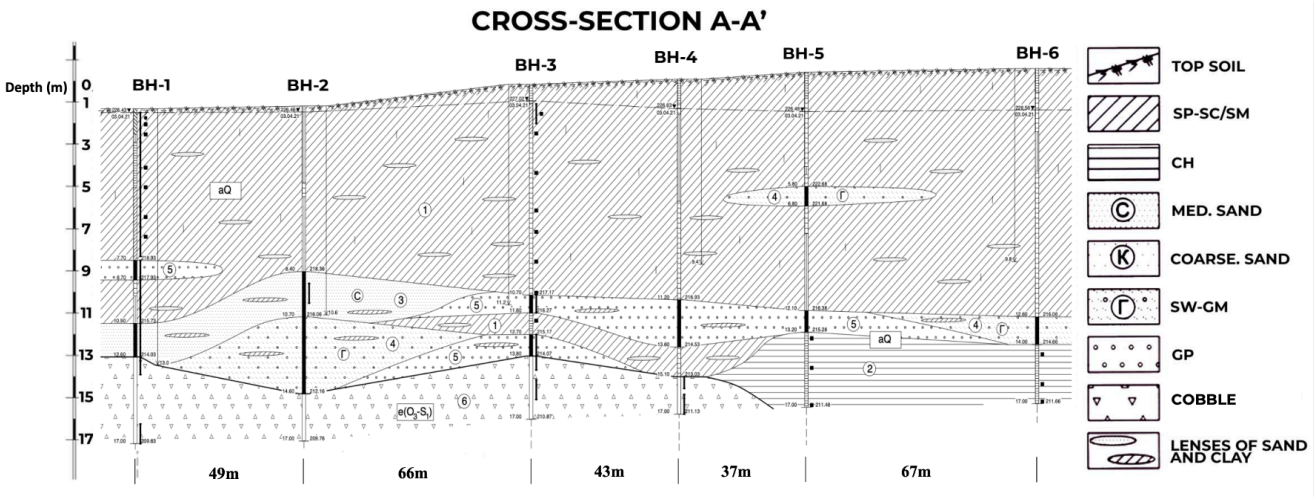

Figure 3-1 Cross section of Site A

Topsoil: This uppermost layer of soil contains fill soil and organic matter.

Layer 1: Poorly graded Sand with Silt and Clay (SP-SC/SM). The initial layer is distinguished by its dark brown coloration and consists predominantly of sand with silt and clay. It has inclusions of medium-sized sand lenses. This layer has variable thickness, ranging from 5.60 to 12.90 meters.

Organic matter content fluctuates between 3% to 10%. According to cone penetration testing, resistance values span from 0.76 to 25.0 MPa, with an average of 4.87 MPa, while soil resistivity on the side surface varies from 33 to 134 kPa, averaging at 90 kPa.

Layer 2: High Plasticity Clay. Layer 2 is distinguished by its cohesive and highly compacted nature, exhibiting a smooth texture and a dark brown to gray coloration. It typically has a thickness ranging from 1.5 to 2 meters. The soil density of the high plasticity clay layer is measured around 2.10 g/cm³. It displays a specific cohesion of 8 kPa and an internal friction angle of 20 degrees. The deformation modulus of this layer is approximately 25 MPa. Cone penetration testing results reveal resistance values ranging from 5.5 to 20 MPa, with an average resistance of 12 MPa. Soil resistivity on the side surface ranges from 150 to 270 kPa, highlighting the compactness and impermeability of this clay layer.

Layer 3: Medium Coarse Sand. Layer 3 is identified by its brown color and the presence of silt and clay lenses and interlayers. The thickness of this layer exhibits significant variation, between 0.50 to 3.00 meters. Soil density is 1.92 g/cm³. Specific cohesion of 2 kPa and an internal friction angle of 35 degrees, with a deformation modulus of 17.0 MPa. According to cone penetration testing resistance values range between 2.50 to 13.9 MPa, averaging 8.62 MPa, and soil resistivity on the side surface extends from 69 to 172 kPa, with an average of 122 kPa.

Layer 4: Coarse and Gravelly Sand. Layer 4 is characterized by its water-saturated, brown-colored appearance, complemented by the presence of silt and clay lenses and interlayers. This layer's thickness varies significantly, ranging from 0.6 to 2.40 meters. The soil density is measured at 2.00 g/cm³. It exhibits a specific cohesion of 1 kPa and an internal friction angle of 38 degrees, alongside a deformation modulus of 20 MPa. According to cone penetration testing resistance

values show a wide range, from 0.97 to 17.3 MPa, with an average value of 8.41 MPa. Soil resistivity on the side surface is observed to range from 37 to 120 kPa, averaging at 59 kPa.

Layer 5: Gravel. Layer 5 presents itself with a brown, noted for the inclusion of silty sand lenses. The thickness of this gravel layer is observed in segments, with ranges between 0.90 and 1.90m. This layer has a soil density of 2.05 g/cm³. The deformation modulus for this layer is recorded at 23 MPa. According to cone penetration testing, resistance values indicate a range from 0.88 to 25.0 MPa, with an average of 10.55 MPa. Soil resistivity on the side surface spans from 26 to 164 kPa, with an average noted at 88 kPa.

Layer 6: Cobble. This layer is distinguished by its yellow-to-greenish-gray coloration. Its thickness ranges from 2.40 to 5.50 meters. The soil density is higher in this layer is 2.12 g/cm³, with a deformation modulus of 33.0 MPa.

Groundwater was encountered at varying depths across the site, ranging from 0.20 to 3.25 meters. The analysis of soil salinity revealed that the soils within Site A predominantly fall into the non-saline category.

Upon completing the geotechnical investigation of Site A, the construction strategy included installing four precast concrete piles for testing (Figure 3-2). The piles' specific dimensions and attributes are detailed in a Table 3-1.

For the installation of the piles in this area, a Junttan PM25H rig and HHK9A hammer was used. The total mass of the hammer is 13.5tons. with a stroke at maximum rated energy 1.2m. The mass of the striking part of the hammer is 9 tons with a certified impact energy of the hammer 106kNm. The drive head used a 20 cm-thick plywood cushion. The drive cap weighed 790kg.

Table 3-1 Test Piles installed at site A

Precast Concrete Pile with non-pre-tensioned Reinforcement			
Pile_Name	Width (cm)	Length (m)	Bearing Stratum
P-1	30*30	16	Cobble
P-2	30*30	14	SP-SC/SM
P-3	30*30	12	Top of Clay
P-4	40*40	12	GP

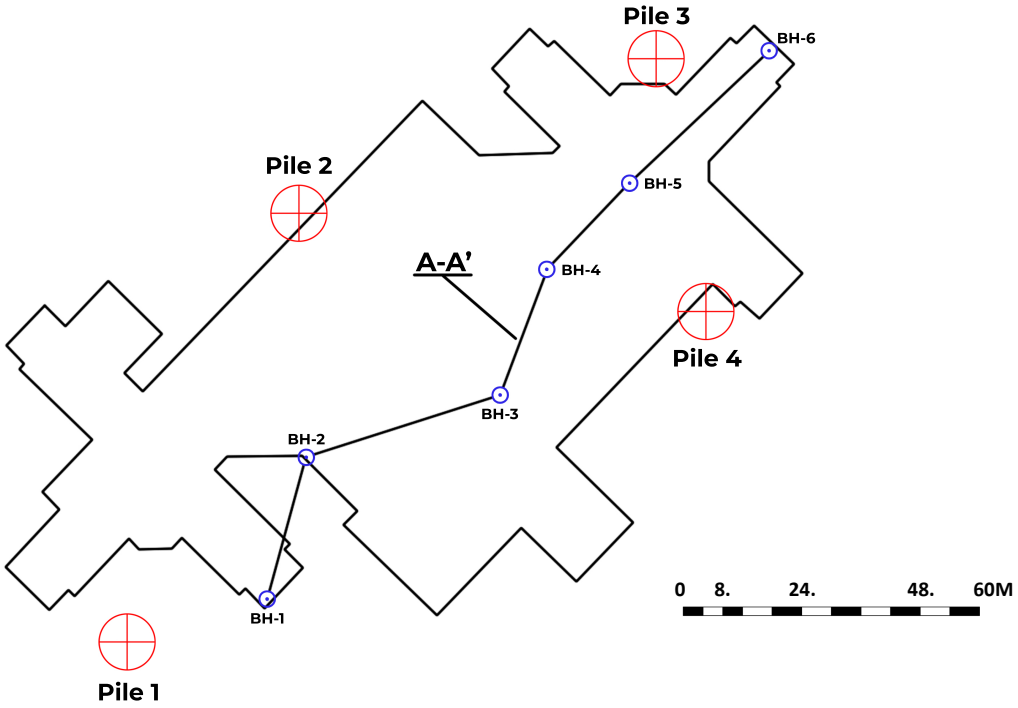

Figure 3-2 Layout of Site A

3.2 Geotechnical Profile of Site B

Site B has been designated for the development of an industrial facility. Subsoil investigation was evidenced by the four detailed boreholes (Figures 3-3 to 3-6) (Geotechnical Survey of the area was done by a Third Party). These boreholes revealed a geologically complex subsurface profile, characterized by layers with Standard Penetration Test (SPT) values exceeding 50 (blows per 45 cm), indicating dense to very dense soil conditions suitable for end-bearing pile foundations. The groundwater level is located 1.5m below the ground surface. Indicator piles were initially driven to validate the pile design and ensure the reliability of the pile installation methods. The production piles were driven after the successful implementation of the indicator piles and their analysis. For the installation of the piles in this area, a Junttan PM25LC rig was used. The total mass of the hammer is 13.5 tons with a stroke at a maximum rated energy of 1.2m. Mass of the striking part of hammer was 8 tons. The certified impact energy of the hammer: 9600kg·m

A cushion of 20cm plywood was used in the drive head. The Weight of the drive cap was 790kg. Locations of the piles and BHs are detailed in Figure 3-7.

BH-1															
Depth		Description	Stratigraphy	Sample		SPT Test						Pocket Penetrometer			
from (m)	to (m)			from	to	15(cm)	7.5(cm)	7.5(cm)	7.5(cm)	7.5(cm)	SPT-N	1st	2nd	3rd	av(tsf)
0	4.8	Sand		0.75	1.25	2	1	1	1	1	4				
				1.5	1.95	2	1	1	1	1	4				
				2.35	2.8	2	1	1	1	1	4				
				3	3.45	3	2	2	2	3	9				
				4	4.45	8	4	6	5	7	22				
4.8	5.8	Silty Sand		5	5.45	6	5	5	8	9	27				
5.8	9.5	clay		6	6.26							4.30	4.80	4.60	4.57
				7	7.45	4	3	5	6	9	23				
				8	8.24							2.80	3.10	3.00	2.97
				9	9.45	7	6	8	7	8	29				
9.5	12.1	Silty Sand		9.9	10.35	20	21	22	7		>50				
				10.55	11.4	11	10	7	11	12	40				
12.1	18	Marl		12.4	12.85	50					>50				
				13.95	14.4	17	14	28	8		>50				
				15.3	15.75	11	15	18	17		>50				
				17	17.45	20	28	22			>50				
18	19.5	Silty Sand		18.4	18.85										
19.5	24.5	Clay		20	20.28							3.30	2.60	2.90	2.93
				21.5	21.95	8	7	8	10	4	29				
				23	23.45	6	9	10	11	4	34				
				24.4	24.59							3.90	3.30	3.50	3.57

Figure 3-3 BH-1

BH-2															
Depth		Description	Stratigraphy	Sample		SPT Test						Pocket Penetrometer			
from (m)	to (m)			from	to	15(cm)	7.5(cm)	7.5(cm)	7.5(cm)	7.5(cm)	SPT-N	1st	2nd	3rd	av(tsf)
0	6	Sand		0.5	0.95	1	1	2	1	1	5				
				1	1.45	1	2	2	1	1	6				
				1.5	1.95	3	2	1	2	1	6				
				2.45	2.9	4	2	2	2	3	9				
				3.25	3.7	4	4	4	3	2	13				
				4.25	4.7	4	3	3	4	3	13				
				5.25	5.7	10	8	10	7	5	30				
6	9	Clay		6.25	6.43							4.00	3.80	3.80	3.87
				7.25	7.7	7	5	7	9	12					
				8.25	8.7	12	8	10	13	19	>50				
9	11.2	Silty Sand		9.25	9.67	20	18	20	12		>50				
				10.25	10.7	15	10	20	10	10	>50				
11.2	12.4	Marl		11.5	11.65	50					>50				
12.4	18.3	Silty Sand		13	13.45	25	20	10	15	5	>50				
				14.5	14.87	19	15	30	5		>50				
				16	16.3	30	20	30			>50				
				17.5	17.65	50					>50				
18.3	25.3	Clay		19	19.3							3.00	2.80	3.00	2.93
				20.5	20.95	11	7	9	10	11	37				
				22	22.17							6.00	5.00	4.60	5.20
				23.5	23.95	11	7	7	8	8	30				
				25	25.3							6.60	5.60	5.80	6.00

Figure 3-4 BH-2

BH-3															
Depth		Description	Stratigraphy	Sample		SPT Test						Pocket Penetrometer			
from (m)	to (m)			from	to	15(cm)	7.5(cm)	7.5(cm)	7.5(cm)	7.5(cm)	SPT-N	1st	2nd	3rd	av(tsf)
				0.4	0.85	1	1	1	1	1	5				
				1	1.45	2	1	1	2	2	8				
				1.5	1.95	4	3	2	1	1	11				
				2	2.45	3	3	4	3	3	16				
				3.25	3.7	7	6	9	13	12	47				
				4.25	4.7	13	9	10	13	14	59				
0	5.7	Sand		5	5.45	8	6	7	10	12	43				
				6.25	6.54							4.00	4.00	4.20	4.10
				7.25	7.7	7	7	8	9	11	42				
				8.25	8.72							4.00	3.20	4.00	3.70
5.7	9.9	Clay		9.25	9.7	3	3	4	5	7	22				
				10.25	10.7	5	5	6	8	7	31				
9.9	12.8	Silty Sand		11.5	11.95	25	50				>50				
12.8	14	Silty Sand		13	13.3							6.00	5.00	5.20	5.40
				14.5	14.95	50					>50				
				16	16.45	30	45	5			>50				
14	18.7	Marl		17.5	17.95	50					>50				
				19	19.3							3.00	3.20	3.00	3.10
				20.5	20.95	10	6	9	9	10	34				
				22	22.3							5.00	5.60	6.20	5.60
				23.5	23.95	20	10	8	6	9	33				
18.7	25.25	Clay		25	25.25							3.00	3.80	3.20	3.33

Figure 3-5 BH-3

BH-4															
Depth		Description	Stratigraphy	Sample		SPT Test						Pocket Penetrometer			
from (m)	to (m)			from	to	15(cm)	7.5(cm)	7.5(cm)	7.5(cm)	7.5(cm)	SPT-N	1st	2nd	3rd	av(tsf)
				0.5	0.95	2	1	1	1	1	4				
				1.25	1.7	2	2	2	3	2	11				
				2	2.45	2	3	3	2	3	13				
				2.75	3.2	3	3	5	6	8	25				
				3.5	3.95	5	8	10	10	9	42				
				4.5	4.95	4	8	9	11	11	43				
0	6.15	Sand		5.5	5.95	5	7	10	11	10	43				
				6.5	6.73							6.30	6.50	7.00	6.00
				7.5	7.95	5	4	6	7	7	24				
				8.5	8.73							7.30	7.50	7.50	7.43
				9.5	9.95	6	5	5	4	5	19				
6.15	10.9	Clay		10.5	10.82							4.00	5.00	5.00	4.67
10.9	13.1	Silty Sand		12	12.45	15	30	20			>50				
				13.5	13.95	50					>50				
13.1	15.6	Marl		15	15.45	50					>50				
15.6	17.2	Silty Sand		16.5	16.95	20	35	15			>50				
17.2	18.7	Marl		18	18.45	25	37	13			>50				
				19.5	19.74							4.00	5.00	4.00	4.33
				21	21.45	6	5	5	7	6	23				
				22.5	22.85							6.00	6.00	7.00	6.33
18.7	24.45	Clay		24	24.45	7	7	8	7	7	29				

Figure 3-6 BH-4

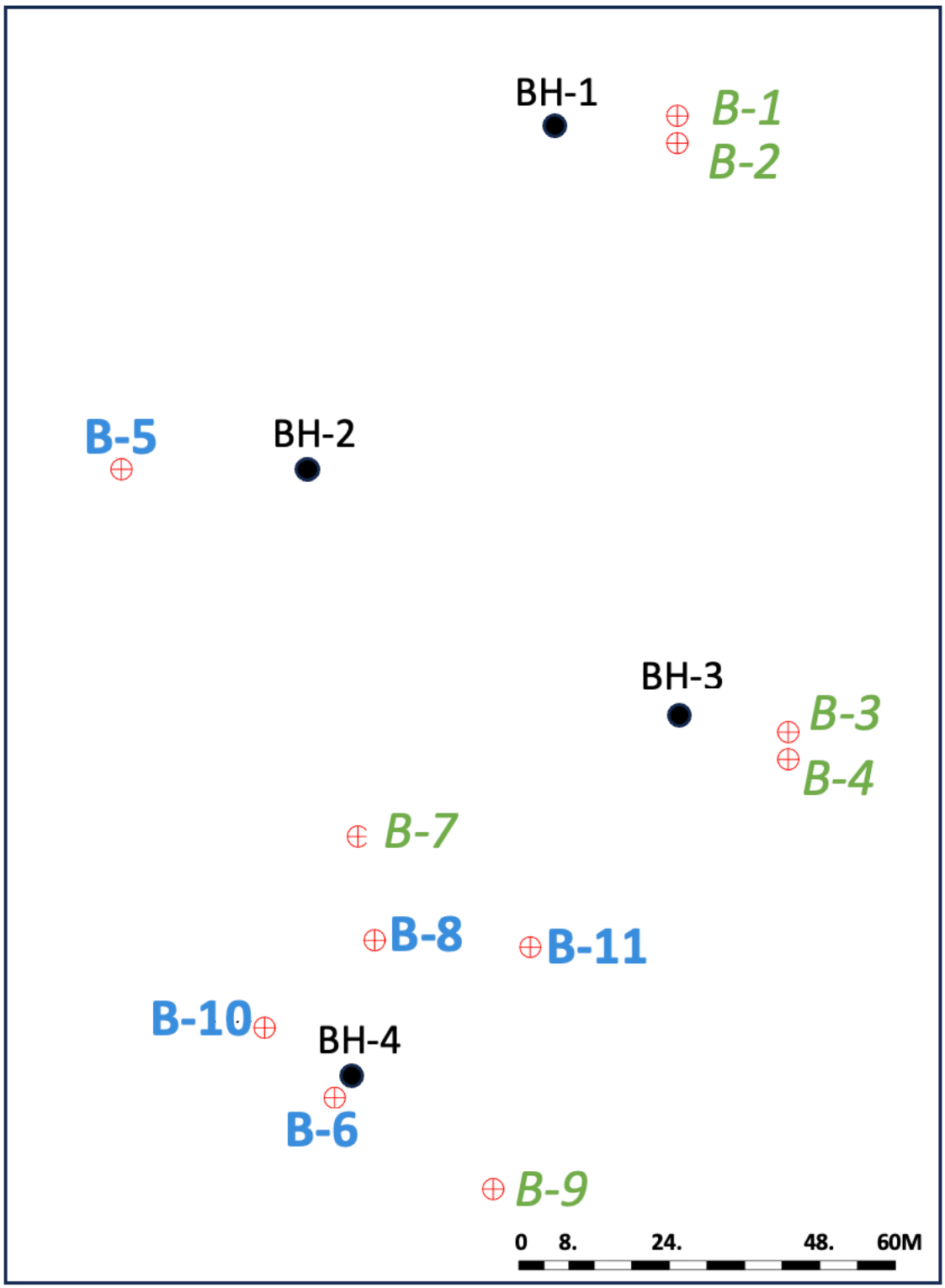

Figure 3-7 Pile Sketch used at Site B

4. Chapter 4

4.1 Introduction

Chapter 4 of the thesis delves into the systematic data collection and analytical methodologies underpinning this research. The dataset comprises PDF documents containing the results of static load tests and PDA across two designated sites. Third-party specialists conducted the Pile Dynamic Analysis and Static Load Testing at Site A and Site B. My role was focused on the detailed analysis of the outcomes of these tests, leveraging the data collected to assess and compare the performance of piles.

Site A provided a comprehensive suite of eight documents, equally divided between Static Load Tests and PDA assessments. The Static Load Tests were executed to the point of failure, yielding a rich dataset that elucidates the piles' ultimate capacities. In parallel, PDA assessments on corresponding piles offered a comparative dataset crucial for evaluating the relative effectiveness of these methodologies in assessing pile performance.

Site B's dataset comprised eleven piles, with five subjected to Static Load Testing and six to PDA evaluations. The initial phase involved the installation and PDA assessment of four indicator piles at the End of Initial Driving (EoD) and after a 20-minute restrike (RD_20min), followed by the PDA evaluations of two production piles. Additionally, the Static Load Test component at Site B tested four piles to failure, while one pile was assessed under a safety factor of two, underscoring a systematic approach to validate pile performance under increased load conditions.

The Data Analysis section critically examined the efficacy of PDA testing methodologies. CAPWAP results were stringently filtered, with match qualities below five deemed reliable for analysis, while those exceeding five were discarded to maintain analytical precision. The

investigation then concentrated on key performance metrics such as EMX (maximum transferred energy) and mobilized settlement, which are critical for assessing energy transfer efficiency during pile driving and the resulting settlement behaviors.

A detailed chronological mapping of pile installation and subsequent Static Load Testing and PDA testing was conducted to elucidate the time-dependent behavior of piles and the evolving characteristics of soil-pile interactions. A comparative evaluation of pile capacities complemented this temporal analysis determined through Static Load Testing and PDA, with static load capacities interpreted using the Kazakh building code and Davisson's criteria.

The insights derived from this analysis are poised to significantly inform best practices in pile testing and installation, with a particular emphasis on the geotechnical engineering landscape in Kazakhstan.

4.2 Pile Static Load Testing

4.2.1Methods

Quick Load Testing Method

At Site A, the Static Load Testing of three piles (P-1, P-2, P-3) was executed using the Quick Load Testing method prescribed by GOST 5686. This approach entails the application of load in equal increments, each constituting 20% of the pile's design load, over 15-minute intervals. Time, load, and displacement readings were captured every minute during the test, providing a detailed profile of pile behavior under load. The test culminated upon encountering a plunging failure, characterized by the necessity for continuous load application to sustain the test load. After this failure, the load was promptly dissipated.

Maintained Load Testing Method

Conversely, Site B's Static Load Testing adhered to the Maintained Load Testing (MLT) method, as prescribed by GOST 5686 and ASTM D1143. This methodology stipulates maintaining the load until the pile settlement rate diminishes to less than 0.1 mm per hour. If pile movement persists, the design engineer imposes sustaining the load until axial displacement breaches the 15 mm threshold. Additionally, one pile at Site A (P-4) was tested using the MLT method, offering a unique comparative perspective within the same site.

4.2.2 Equipment Used in Static Load Testing

For the loading, a 300-ton (type CLG3006E108) ENERPAC hydraulic jack was mobilized to Site A (Figure 4-1). The jack used is a double-acting hydraulic jack with a stroke of 150 mm and a maximum hydraulic pressure of 700 bar. A kentledge with 250 tons was used as a reaction system. The jack was placed onto a specially fabricated steel pile head cover of 2.5 mm. The space between the pile head and the main beam was bridged with a hydraulic jack, flat steel plates, cylindrical steel plates, and a load cell. The purpose of the steel plates is to separate the jack, loadcell, and cylindrical plates and to overcome the remaining gap between the top of the pile and the main beam. A 300-ton load cell was used. Two wooden support beams were used as reference beams for displacement sensors.

The reference frames, main beam, and loading frame were regularly checked with a digital-level instrument to detect any movements and cross-reference the movement of the pile (Figure 4-2).

Four transducers were employed to measure the pile's displacement. The sensors have a stroke of 400 mm and an accuracy of 0.025 mm.

Specifically designed for static load testing, the SLT2 system allows for remote monitoring of the tests from a distance. This system facilitates real-time data acquisition and minimizes personnel

risk by eliminating the need to be near high-load components. The SLT2 logger gathers load and displacement measurements, processing and automatically transferring the data to a computer (Figure 4-3).

The test setup for Site B is approximately the same as for Site A except for the hydraulic jack. A 300-ton (Type HJ300H15) Holmatro hydraulic jack was mobilized for the loading. The jack used is a double-acting hydraulic jack with a stroke of 150 mm and a maximum hydraulic pressure of 720 bar. A 240-ton Kentledge was used as a reaction system.

Figure 4-1 Enerpac Hydraulic Jack

Figure 4-2 Digital-level instrument. Courtesy of Fugro Kazakhstan

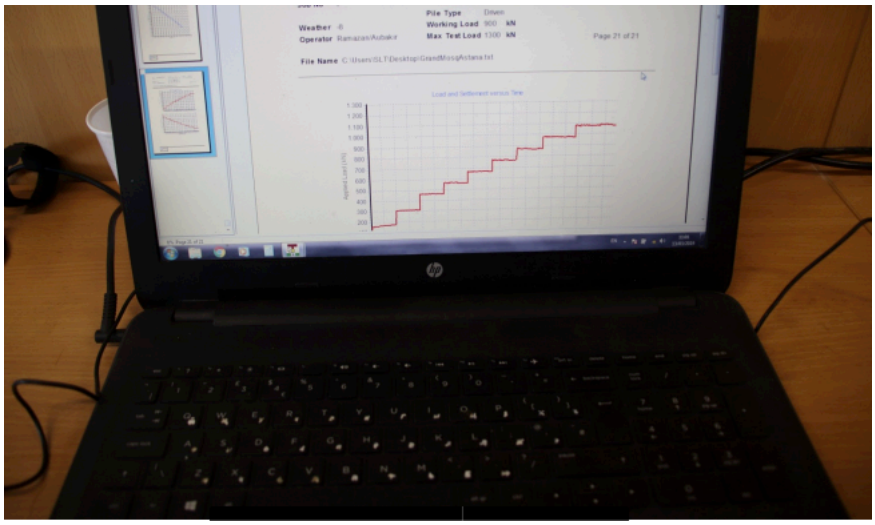

Figure 4-3 SLT2 remote monitoring Program. Courtesy of KGS Astana.

4.3 Pile Dynamic Analysis

Filed measurements consist of a minimum of two strain transducers and two accelerometers at opposite sides of the pile to monitor strain and acceleration and account for non-uniform impacts and bending (Figure 4-4). Sensors are bolted at least two diameters below the pile head and above ground level. Following the attachment of sensors to the pile, the driving process resumes, adhering to standard procedures. Signals from the sensors are transmitted to the Pile Driving Analyzer data acquisition system on site. The PDA 8G, representing the latest generation in dynamic testing technology, was deployed at both sites. During the pile driving operation, the PDA performs real-time integration and computation of the dynamic records and stores data for further interpretation by the Case Pile Wave Analysis Program in an office setting.

Figure 4-4 Sensors bolted to Pile. Courtesy of Keller Central Asia

4.4 Pile Capacity from Static Load Test

Site A

Static pile capacity was determined in piles P-1, P-2, P-3, P-4 (table). Piles P-1 (Figure 4-5), P-2 (Figure 4-6), and P-3 (Figure 4-7) were tested to failure using the Quick Load Test Method. These tests were conducted to record the load-displacement behavior, determining each pile's failure point. The capacities for these piles were interpreted based on the criteria outlined in the Kazakh Building Code (SNiP RK 5.01-01-2002) and the Davison offset limit.

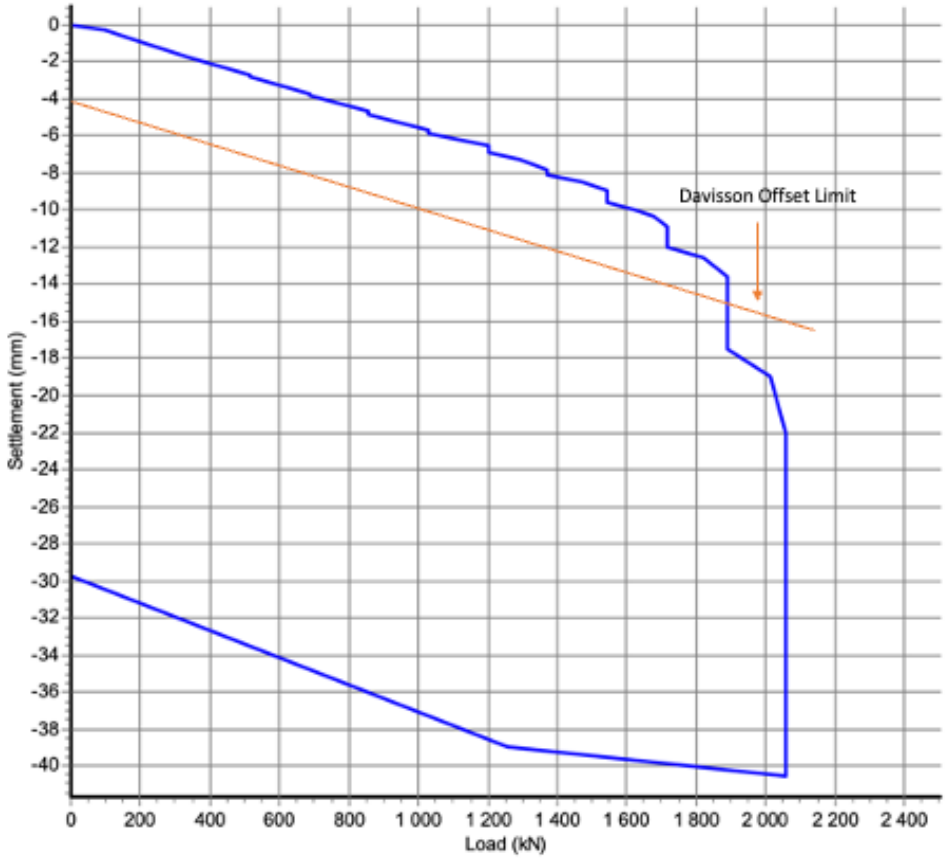

Figure 4-5 Load settlement graph for pile P-1.

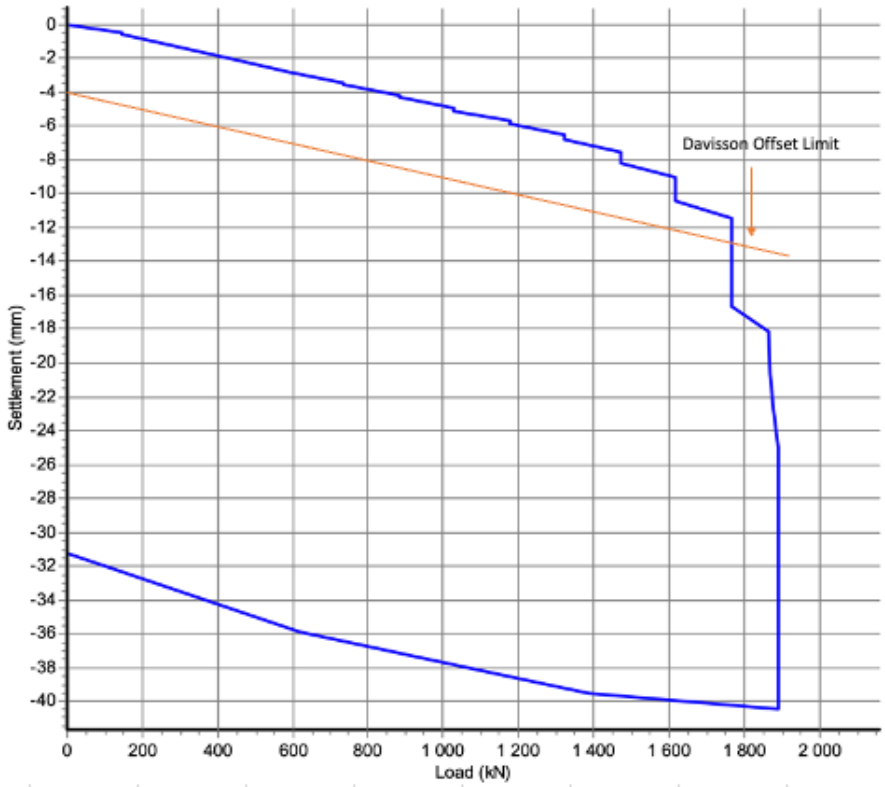

Figure 4-6 Load settlement graph for pile P-2.

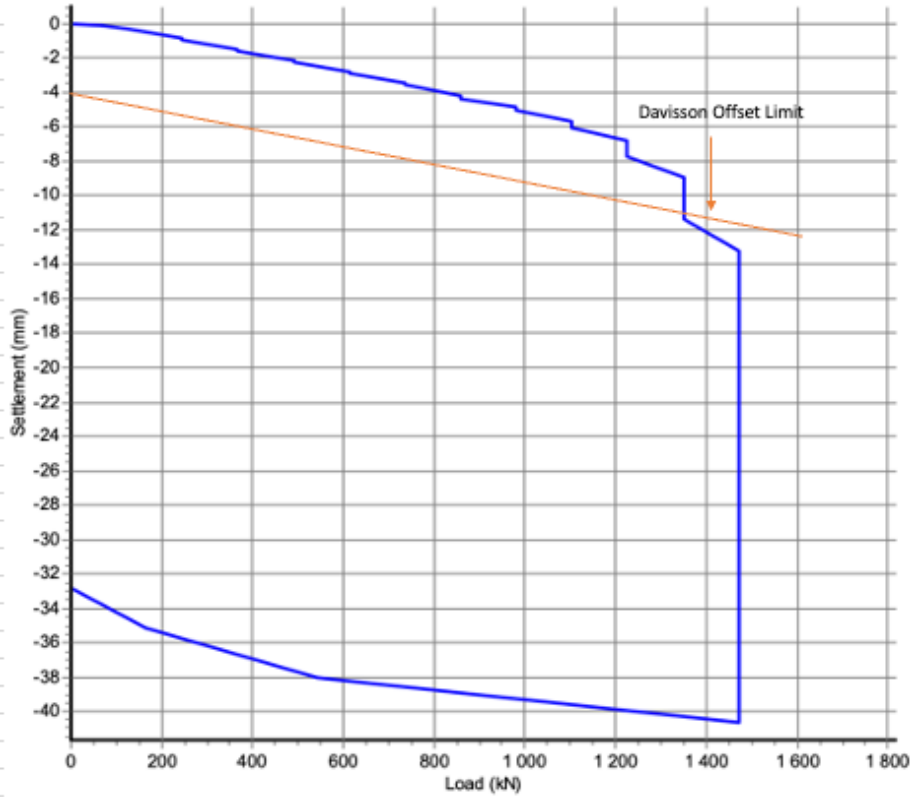

Figure 4-7 Load settlement graph for pile P-3.

Conversely, Pile P-4 (Figure 4-8) was tested with the maintained load test method in 12 steps, including one loading and unloading cycle. The design load of P-4 was 70 tons, and the test load was 2 times the design load, i.e., 140 tons. During testing at Load 1200kN, the pile had a plunging effect with a 35mm permanent settlement. As per the Kazakh Building Code, 1200kN is the ultimate capacity of the pile, and the Davisson offset limit is also 1200kN.

Table 4-1 Static Load Test Analysis for Site A

Pile Name	Date Installed	Date Tested	Capacity by Kazakh Building Code (kN)	Capacity by Davisson Offset (kN)	Length (m)
P-1	4/8/2023	5/16/2023	2050	1880	16
P-2	4/8/2023	5/5/2023	1880	1780	14
P-3	4/8/2023	4/25/2023	1460	1350	12
P-4	4/8/2023	4/28/2023	1200	1200	12

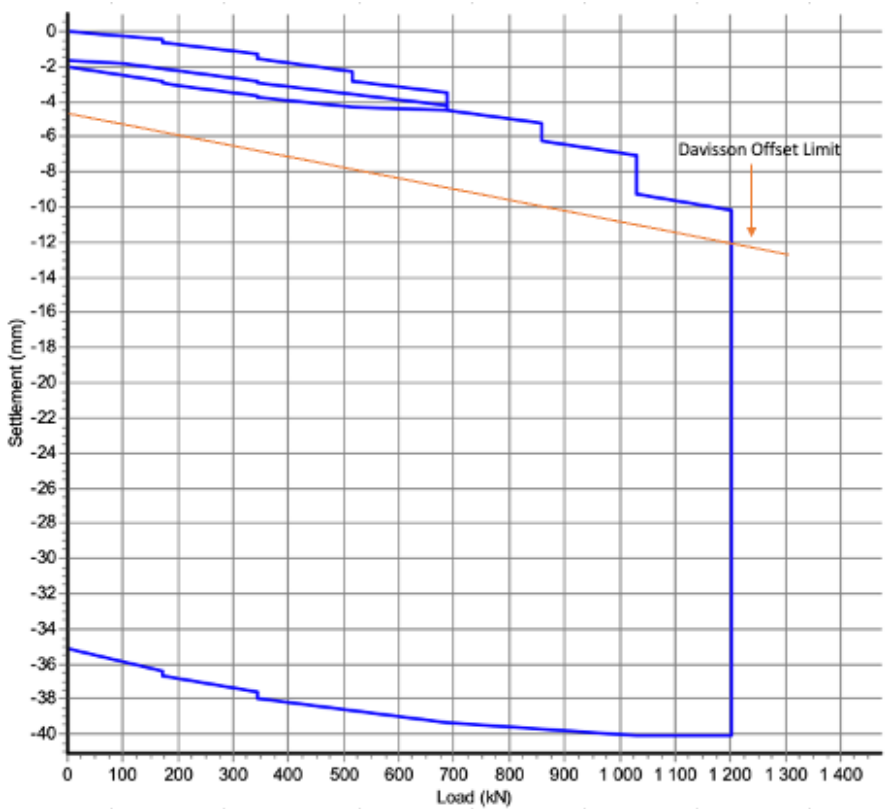

Figure 4-8 Load settlement graph for pile P-4.

Site B

At Site B, the evaluation of precast concrete piles, namely B-5, B-6, B-8, and B-10, was conducted using the Maintained Load Test method, with tests carried to failure to ascertain the ultimate load-bearing capacities. The pile capacity evaluation was guided by the stringent criteria delineated in the Kazakh Building Code (SNiP RK 5.01-01-2002) and with the Davisson offset limit (Figures 4-9,4-10,4-11,4-12).

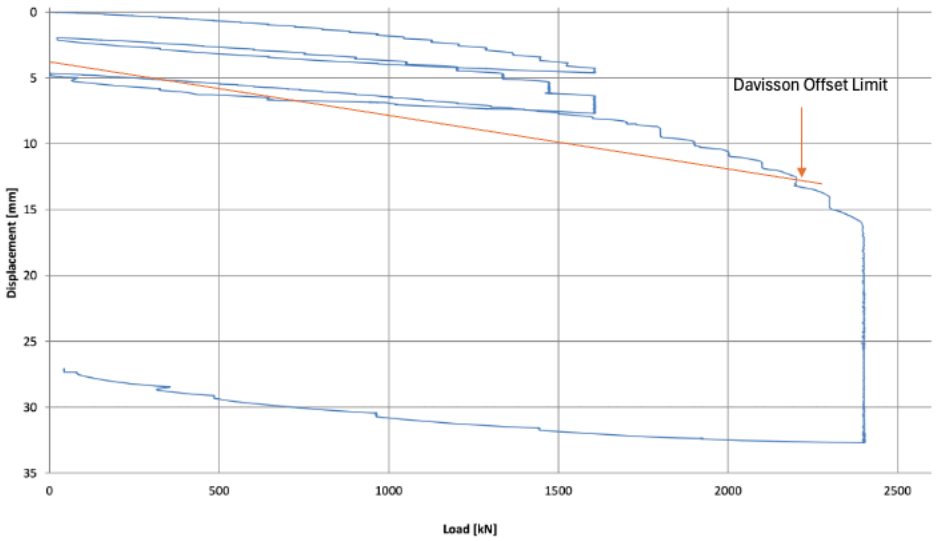

Figure 4-9 Load settlement graph for pile B-5

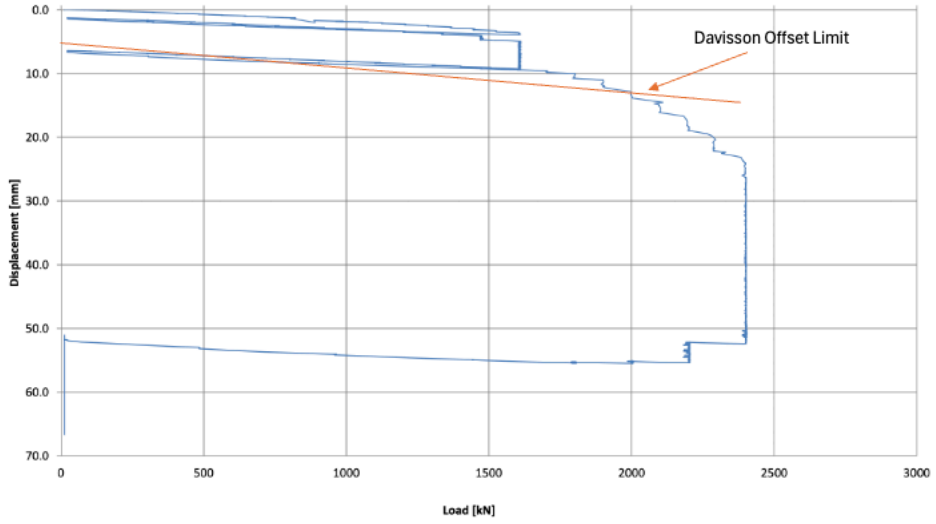

Figure 4-10 Load settlement graph for pile B-6

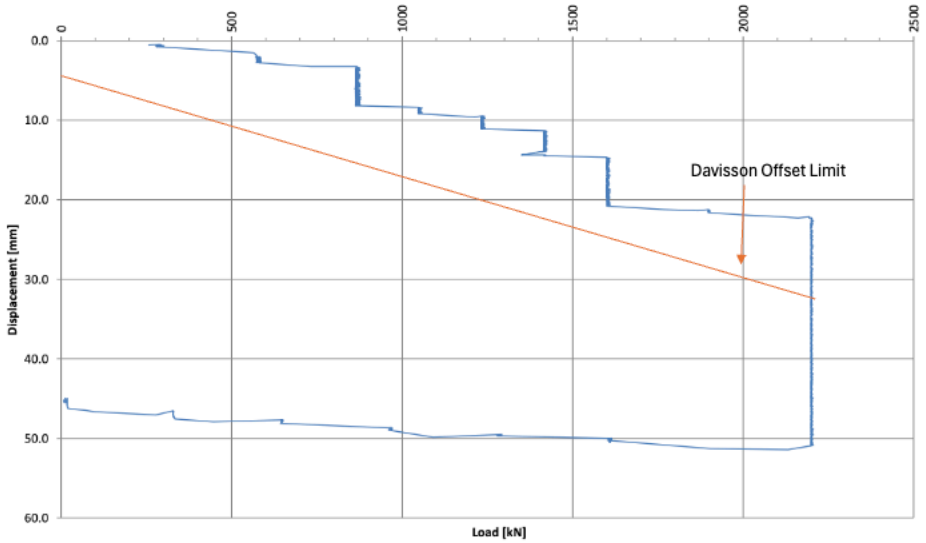

Figure 4-11 Load settlement graph for pile B-8

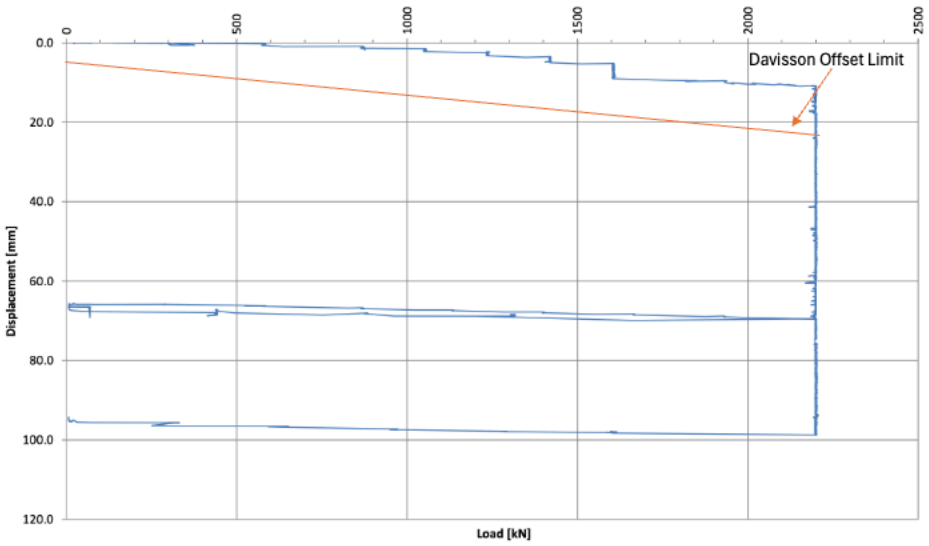

Figure 4-12 Load settlement graph for pile B-10

Additionally, pile B-11, which is located 20m to the east of pile B-8, was tested with a safety factor of two, doubling the design load to assess its performance and capacity. This approach checked the pile's capacity under doubled anticipated loads and provided an opportunity to analyze the elastic behavior and the corresponding slope of the load-settlement curve with those of piles tested to failure.

Table 4-2 Static Load Test Analysis for Site B

Pile Name	Date Installed	Date Tested	Capacity by Kazakh Building Code (kN)	Capacity by Davisson's Offset (kN)	Bearing Stratum
B-5	7/1/2017	8/21/2017	2400	2200	Silty Sand
B-6	6/15/2017	9/25/2017	2200	2000	Marl
B-8	8/20/2015	12/24/2015	2200	2200	
B-10	8/20/2015	12/17/2015	2200	2200	
B-11	9/2/2015	1/13/2016	Out of range	Out of range	

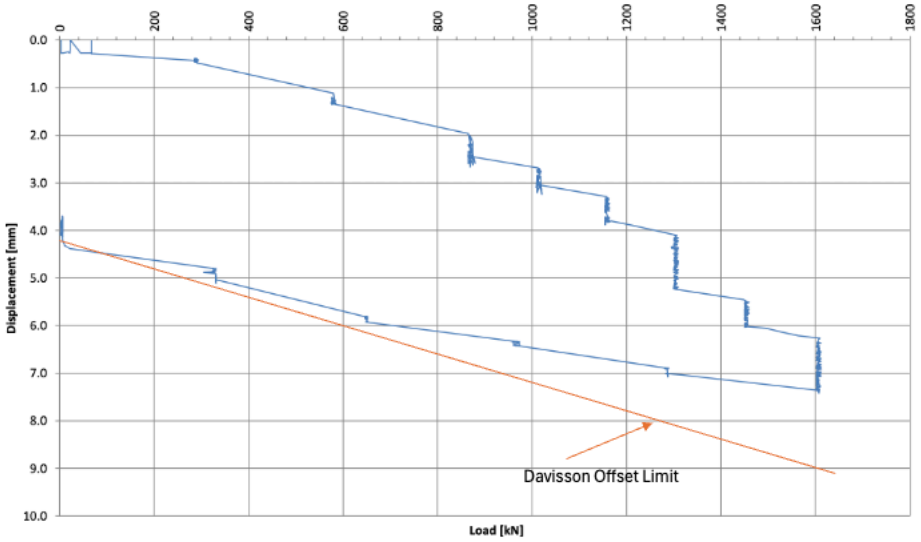

Figure 4-13 Load settlement graph for pile B-11

4.5 Pile Capacity from Pile Dynamic Analysis Method

In the analysis of Site A, Pile Dynamic Analysis (PDA) testing was conducted ten days post-installation to evaluate the piles' performance and capacity. The results of these PDA tests are presented in Figures 4-14, 4-15, 4-16, and 4-17. Details of the mobilized energy and settlement per blow for each pile are presented in Table 4-3**.**

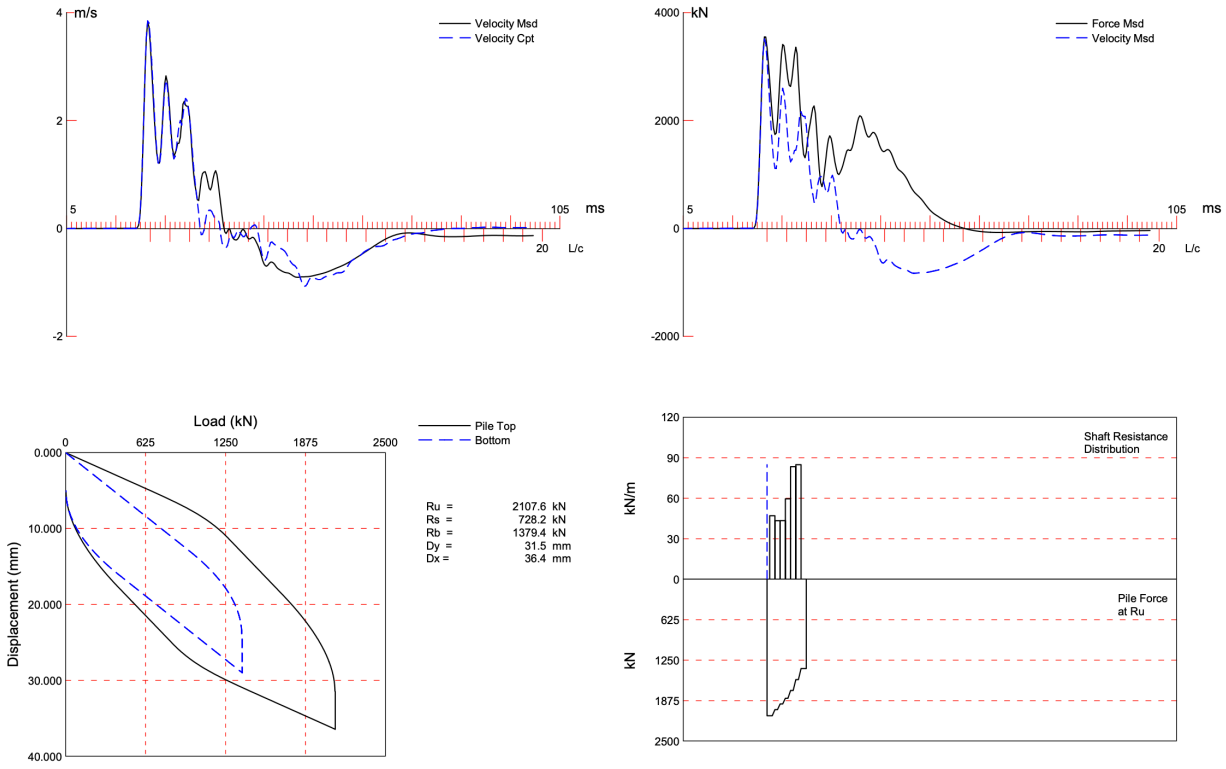

Figure 4-14 CAPWAP Interpretation of P-1

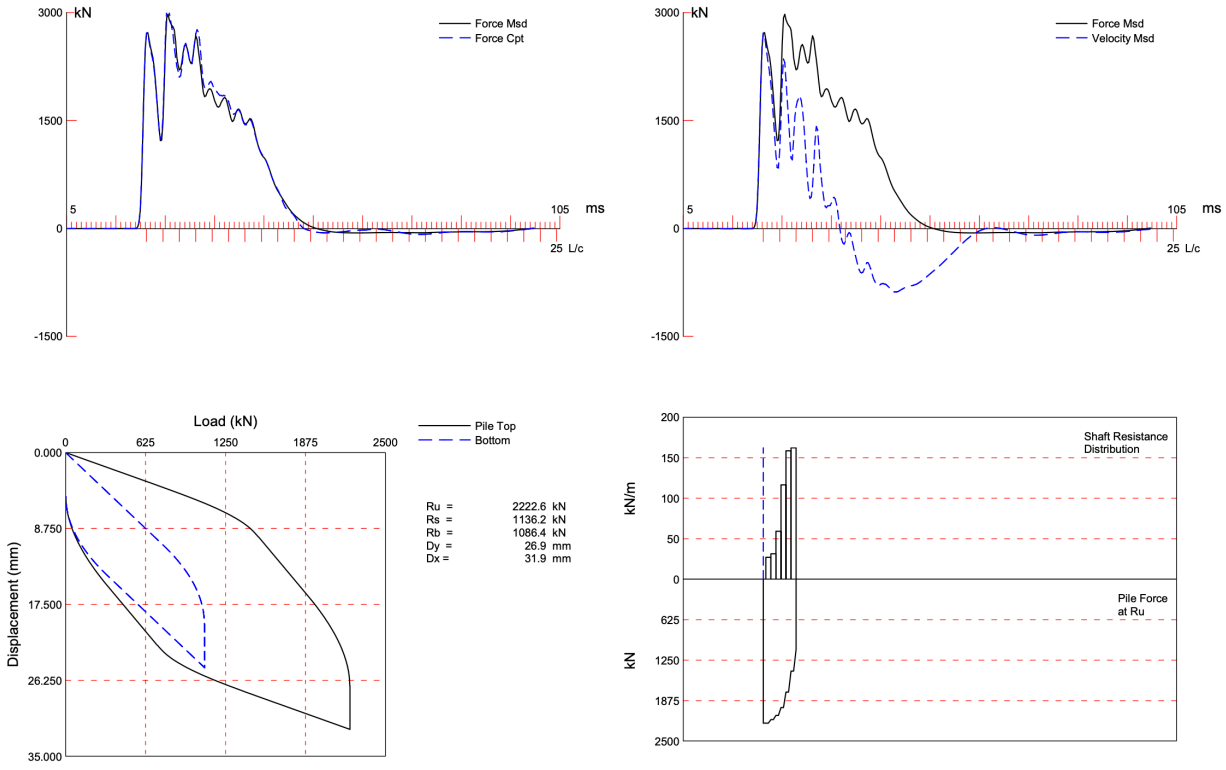

Figure 4-15 CAPWAP Interpretation of P-2

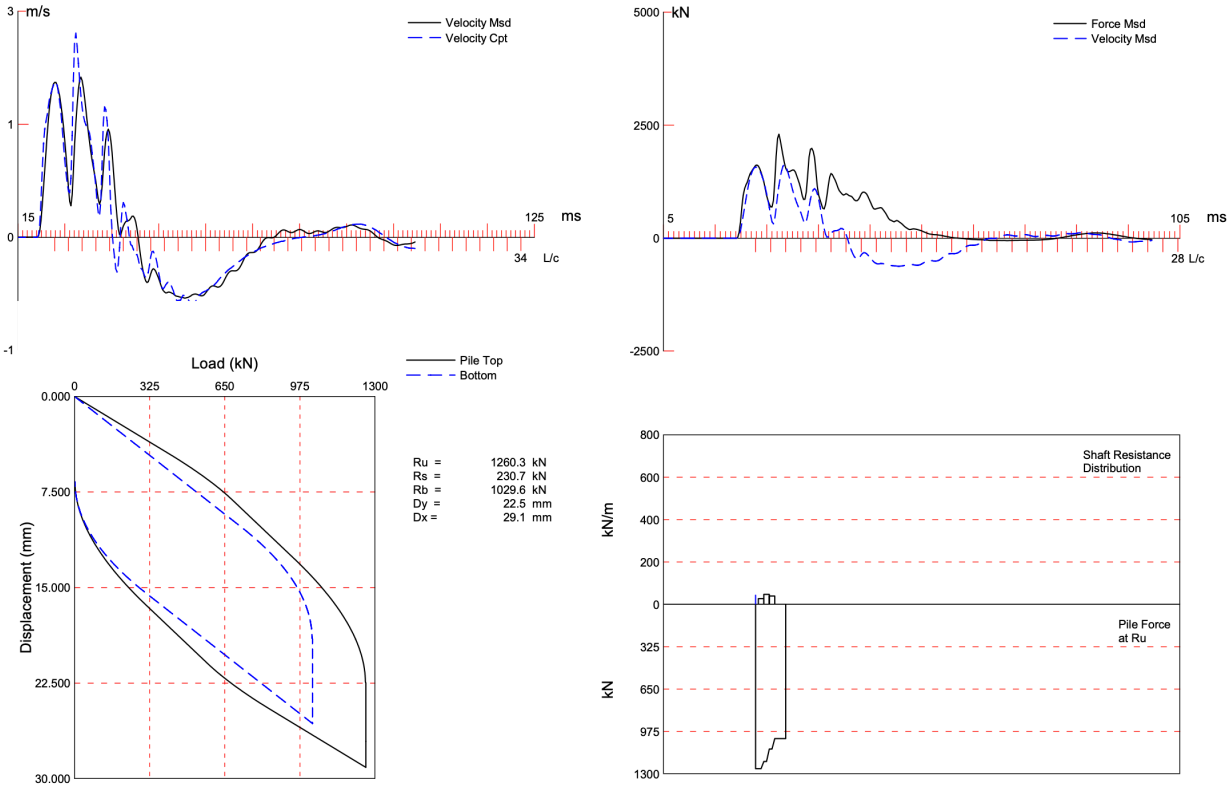

Figure 4-16 CAPWAP Interpretation of P-3

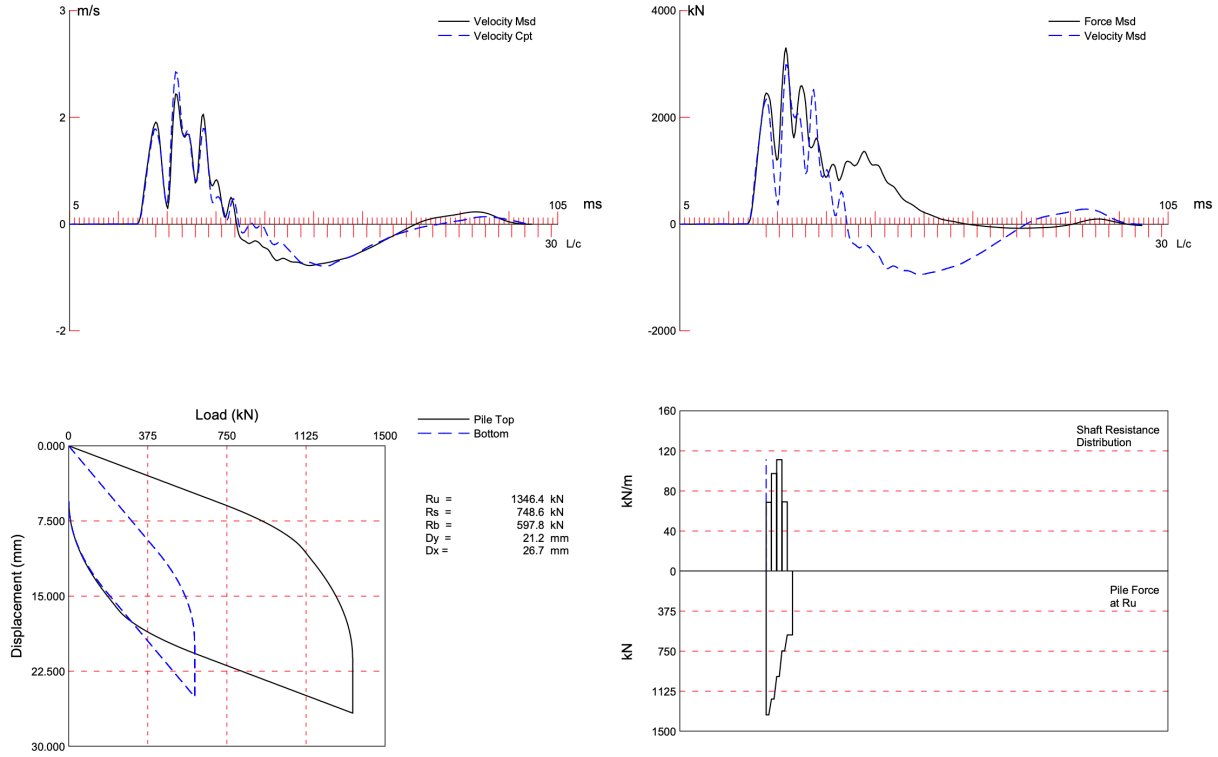

Figure 4-17 CAPWAP Interpretation of P-4

Table 4-3 PDA Testing Results for Site A

Pile_Name	Ins_Date	PDA_Date	Ultimate resistance (kN)	Shaft resistance (kN)	Base Resistance (kN)	Maximum Energy (kJ)	Settlement/Blow (mm)
P-1	4/8/23	4/18/23	2108	728	1380	65.5	5
P-2	4/8/23	4/18/23	2223	1136	1087	52.4	5
P-3	4/8/23	4/18/23	1260	230	1030	25.6	6.6
P-4	4/8/23	4/18/23	1346	748	598	33.1	5.5

In the examination of Site B, PDA testing was performed after the pile installation to assess the piles' behavior and capacity. The outcomes of these PDA evaluations are illustrated across Figures 4-18 to Figure 4-27. Comprehensive data concerning the mobilized energy and the settlement per blow for each tested pile are detailed in Table 4-4.

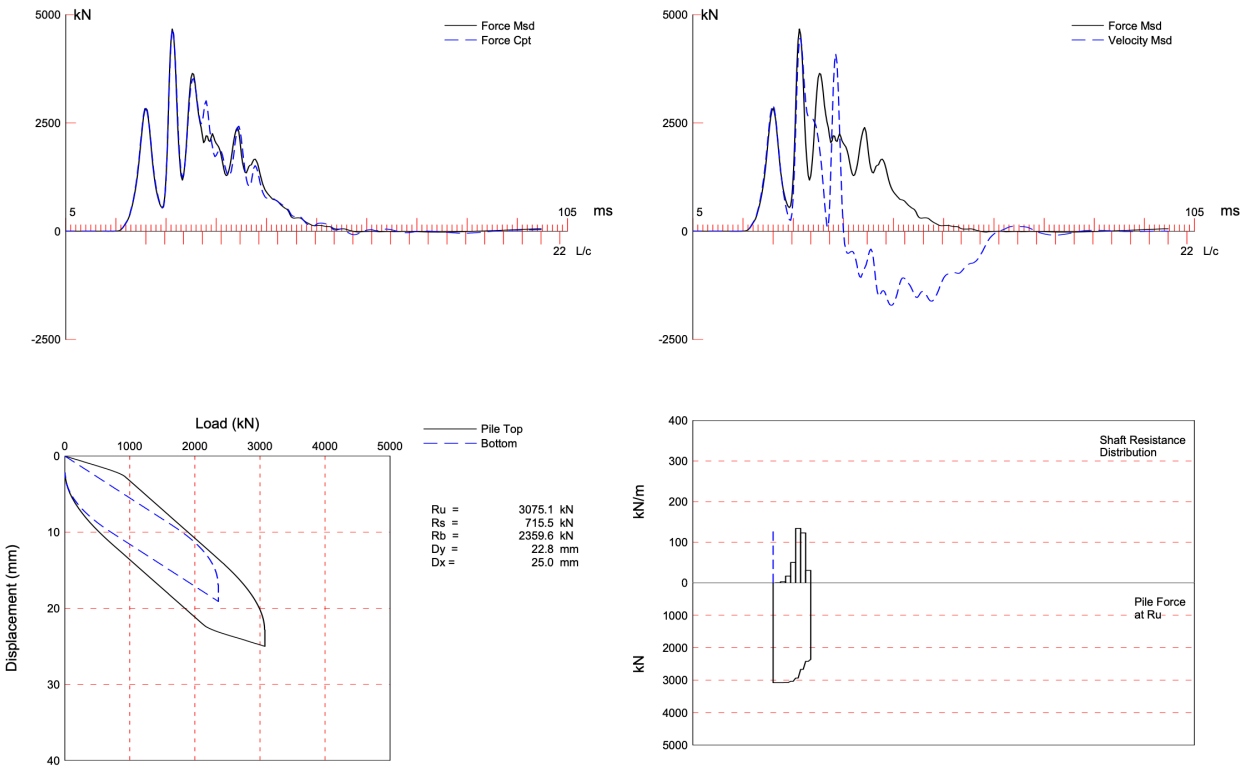

Figure 4-18 CAPWAP Interpretation of Indicator Pile (B-1 Initial Drive)

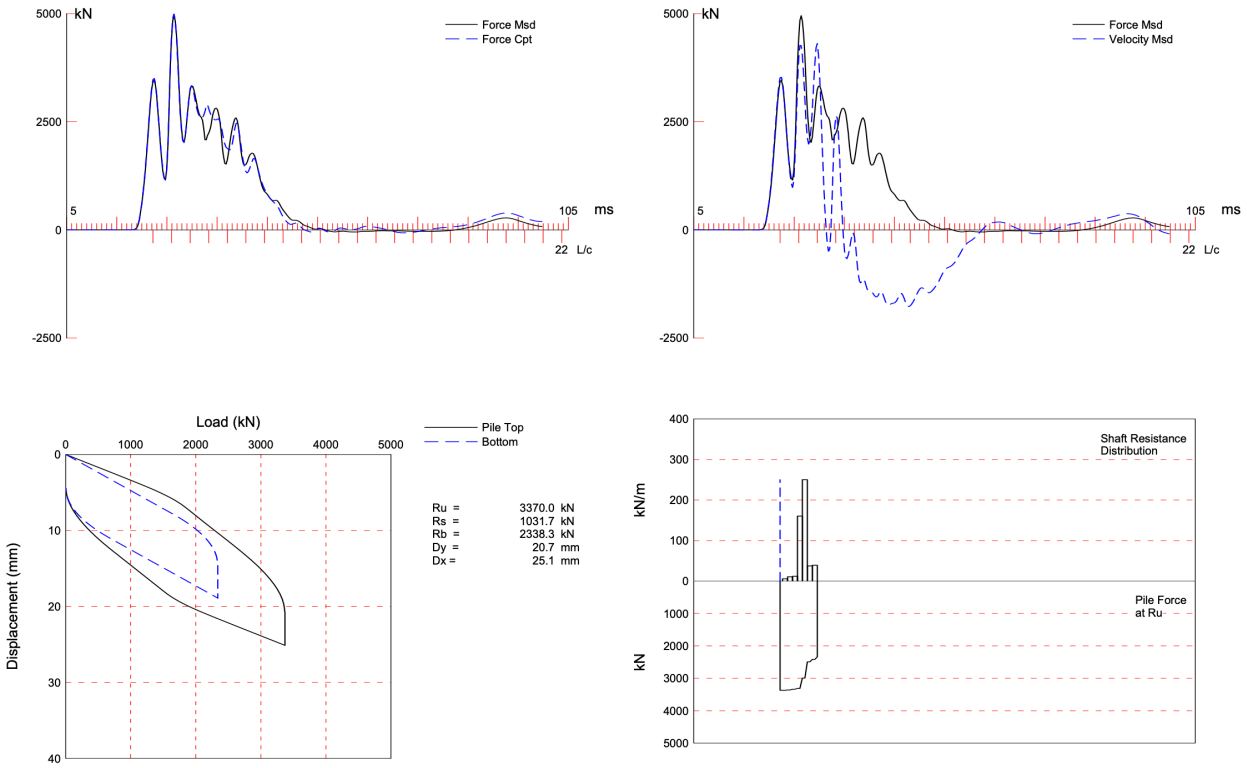

Figure 4-19 CAPWAP Interpretation of Indicator Pile B-1 (Redrive after 20 mins)

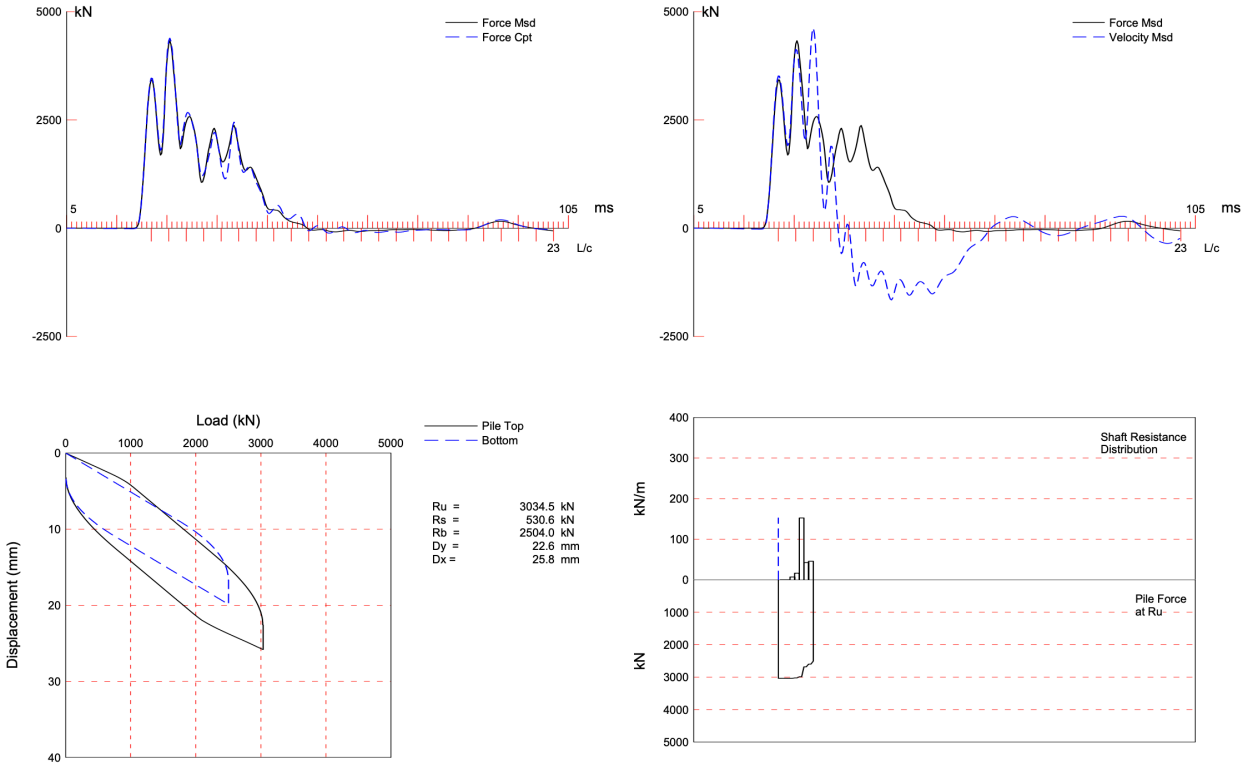

Figure 4-20 CAPWAP Interpretation of Indicator Pile B-2 (Initial Drive)

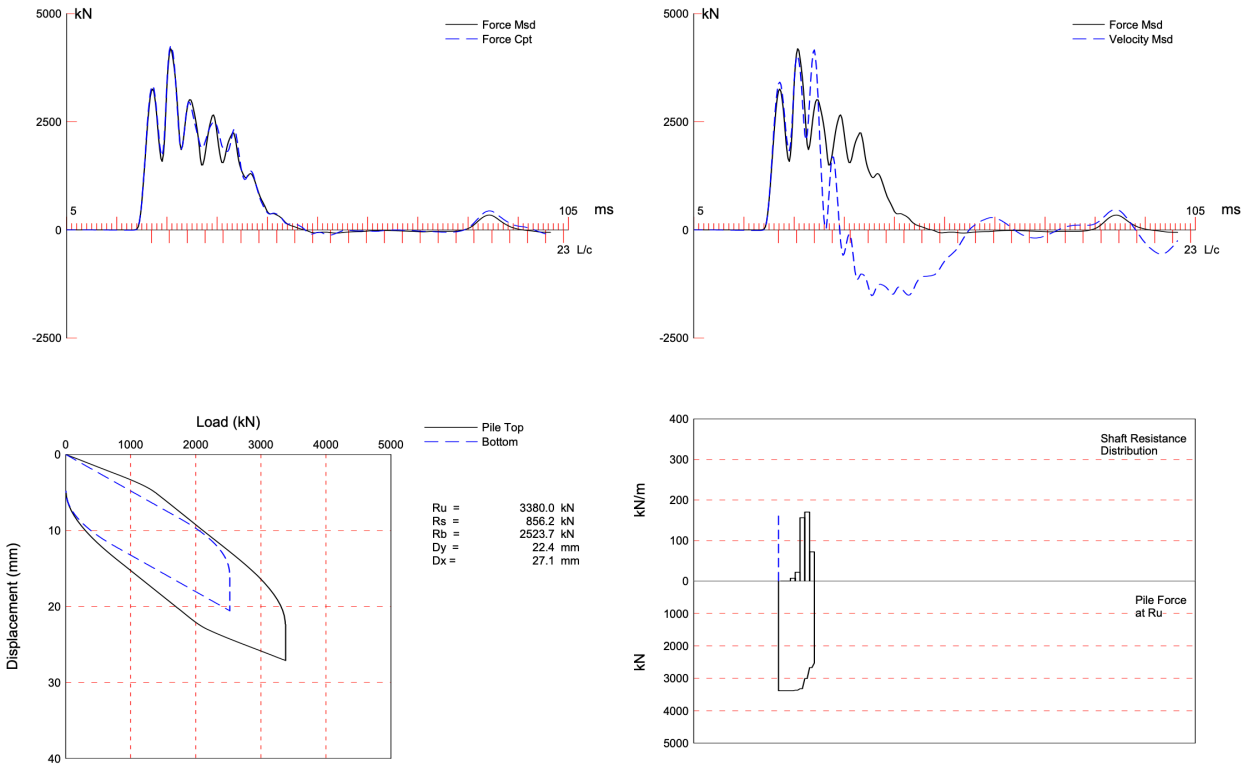

Figure 4-21 CAPWAP Interpretation of Indicator Pile B-2 (Redrive after 20 mins)

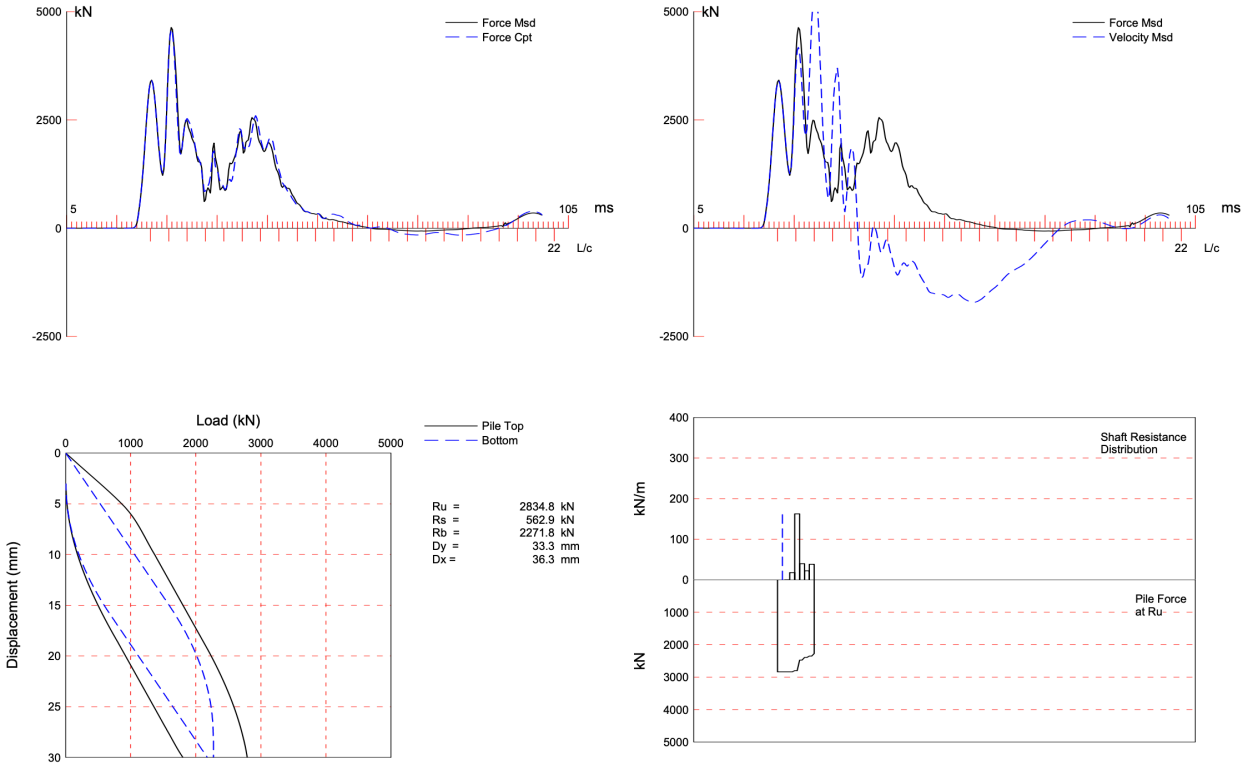

Figure 4-22 CAPWAP Interpretation of Indicator Pile B-3 (Initial Drive)

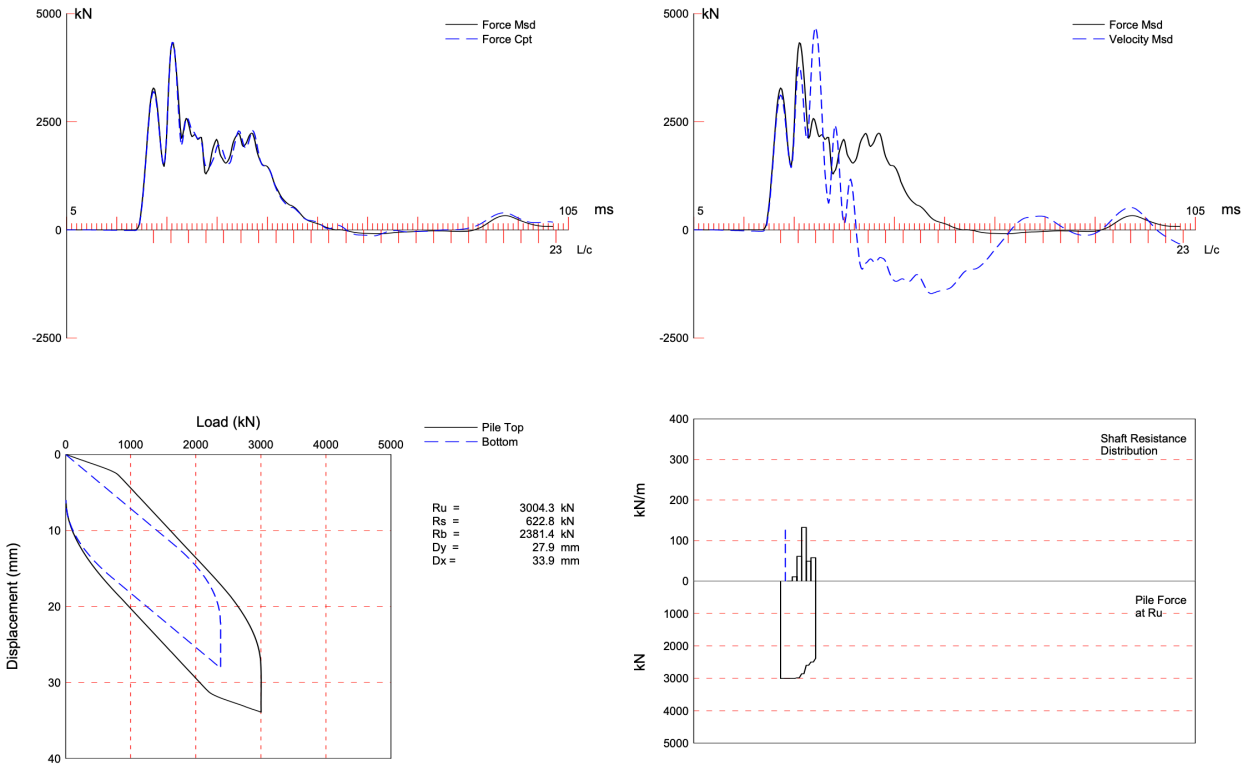

Figure 4-23 CAPWAP Interpretation of Indicator Pile B-3 (Redrive after 20 mins)

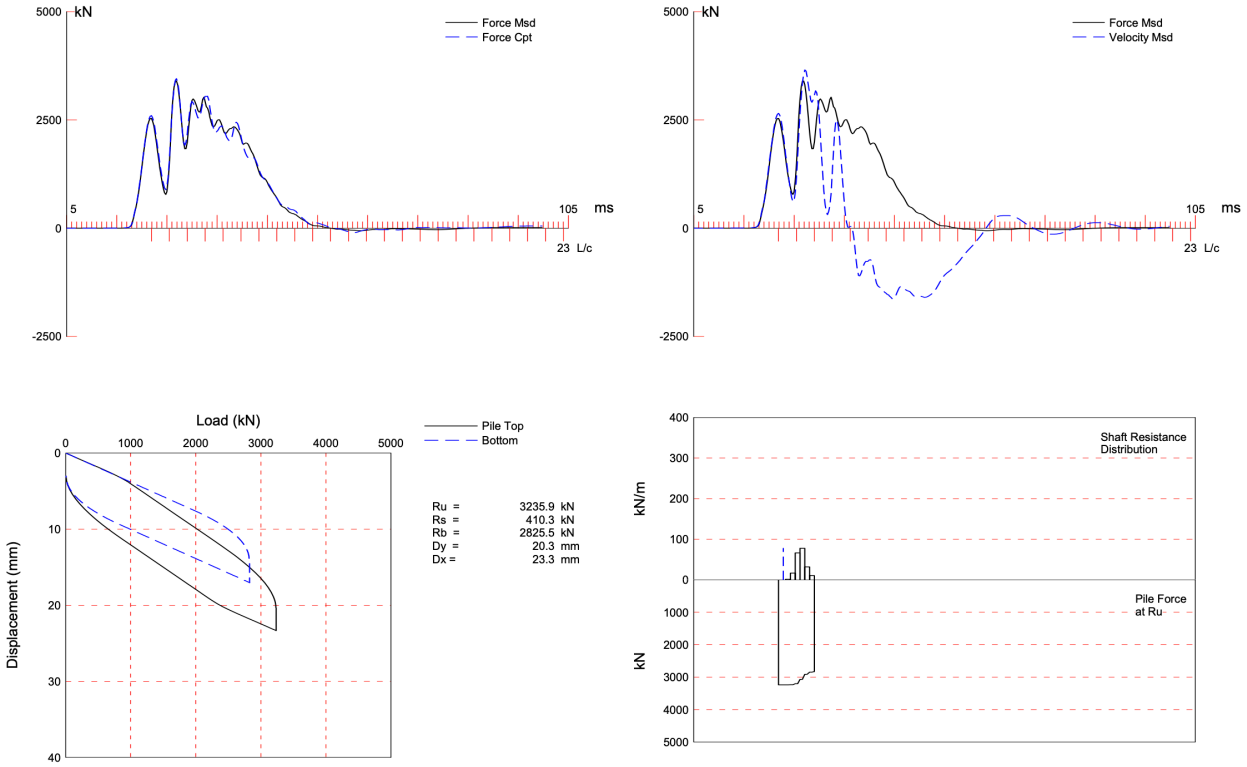

Figure 4-24 CAPWAP Interpretation of Indicator Pile B-4 (Initial Drive)

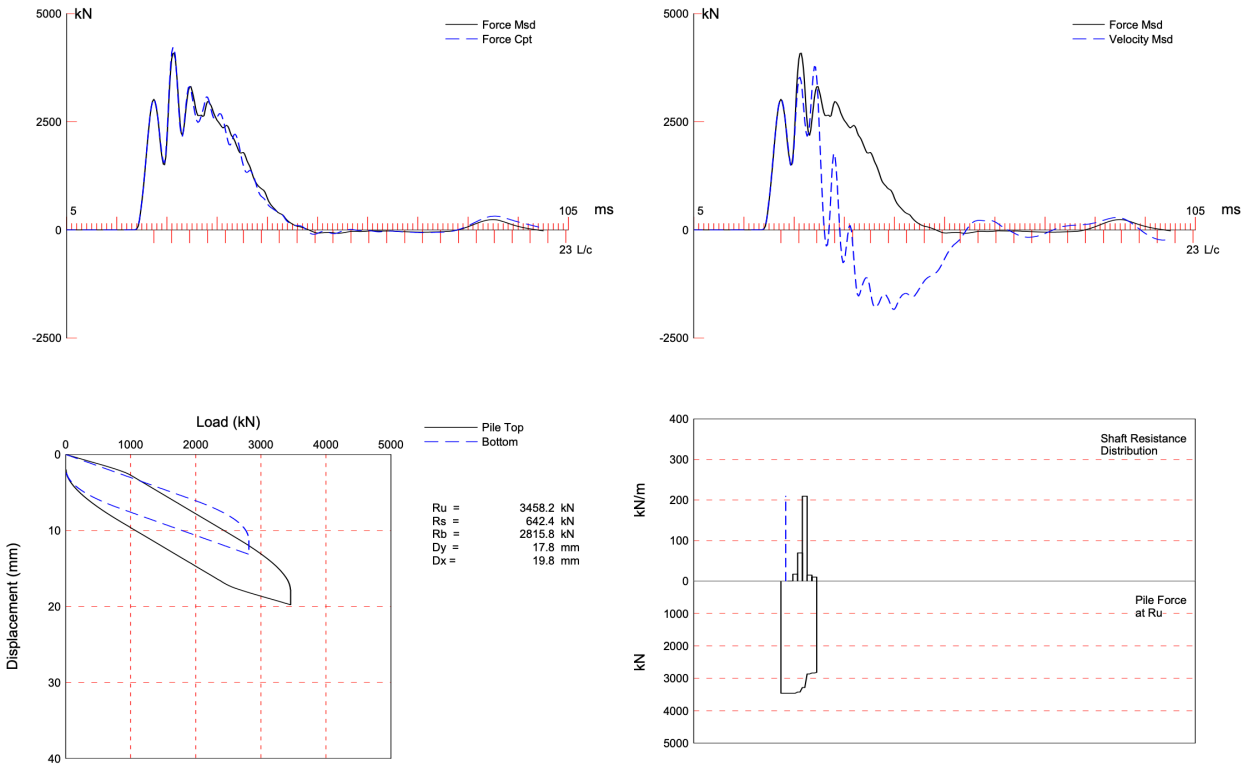

Figure 4-25 CAPWAP Interpretation of Indicator Pile B-4 (Redrive after 20 mins)

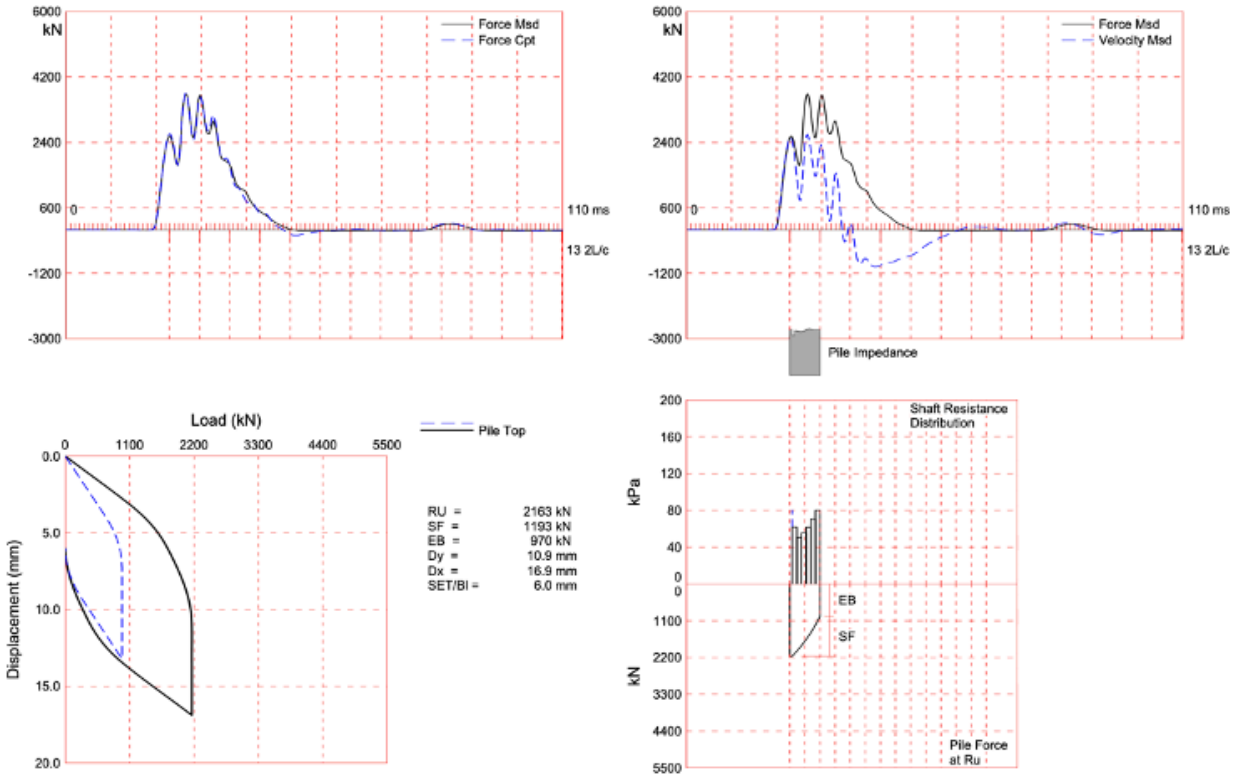

Figure 4-26 CAPWAP Interpretation of Pile B-7

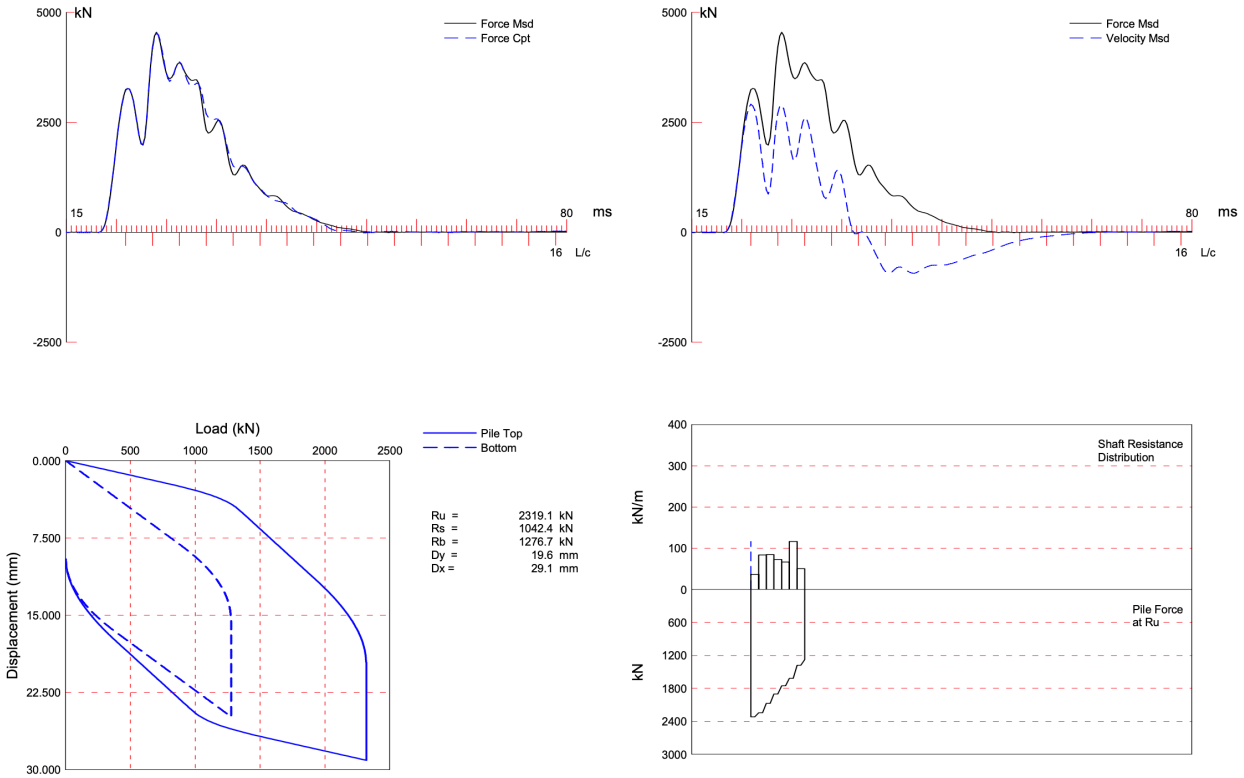

Figure 4-27 CAPWAP Interpretation of Pile B-9

4.6 Pile Capacity Summary and Discussion

At Site A, the geotechnical investigation included both Static Load Testing and Pile Driving Analysis (PDA) tests, with four instances of each method being implemented. The detailed outcomes of these tests, including the assessed capacities and the dates of test execution, are presented in Table 4-4.

Table 4-4 Comparison of Pile Capacities and Test Dates for Site A

Pile_ Name	Length (m)	PDA (kN)	Match Quality	Static (kN)	Davisson (kN)	Pile Installed	PDA Test	Static Test	Ins-PDA (Days)	PDA-Static (Days)
P-1	16	2107	4.55	2050	1880	4/8/23	4/18/23	5/16/23	10	28
P-2	14	2222	3.28	1880	1780	4/8/23	4/18/23	5/5/23	10	17
P-3	12	1260	6.32	1460	1350	4/8/23	4/18/23	4/25/23	10	7
P-4	12	1346	4.83	1200	1200	4/8/23	4/18/23	4/28/23	10	10

Upon examination of the test data, a notable congruence between the capacities determined by the Static Load testing and PDA methods is observed (Figure 4-28). This alignment substantiates the reliability of the PDA method in assessing pile capacities, which is comparable to the traditional Static Load Test approach. Notably, Pile P-1, bearing on a cobble layer, and Pile P-4, on a gravel layer, exhibit PDA results that closely match the static results.

Furthermore, Pile P-2, bearing on SP-SC/SM soil, demonstrates a notably high capacity in PDA compared to static testing. Similarly, Pile P-3, situated on clay, shows a slightly higher capacity in PDA, indicating the enhanced sensitivity of PDA to variations in soil conditions.

Considering the geological consistency and the time elapsed between pile installation and testing, no significant capacity gain was anticipated at Site A. The empirical data showcase consistent capacity measurements across different testing intervals. This consistency underlines the stability of soil-pile interaction and the negligible effect of time on the pile capacity at this site.

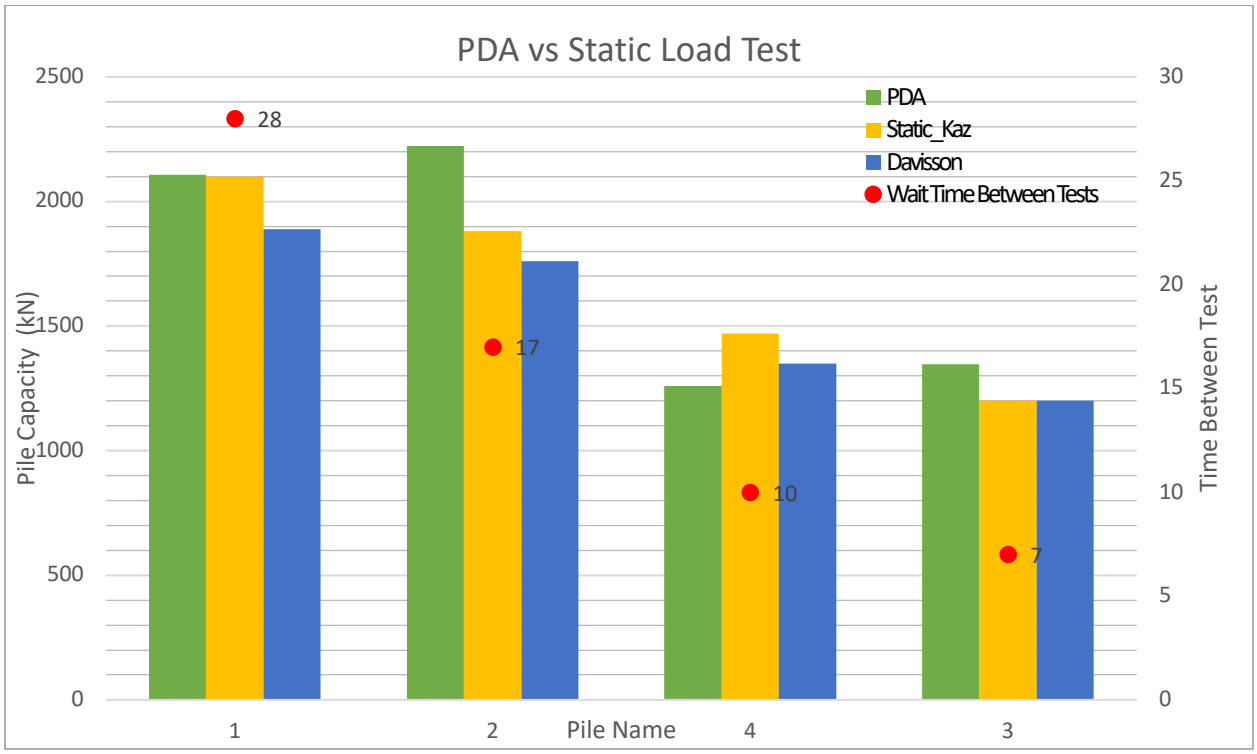

Figure 4-28 Capacity Comparison for Site A

In the static load testing results analysis for Site A, both the Kazakh Building Code and Davisson's offset limit were employed to interpret pile capacities. The comparative analysis revealed a close alignment between the two interpretation methods, with Davisson Criteria demonstrating slightly more conservative results (Figure 4-28). This slight variance underscores the nuanced differences inherent in static load testing interpretation methods. The conservative nature of Davisson's offset limit may be attributed to its specific consideration of pile behavior and safety factors, which tends to result in a more cautious estimation of pile capacity. This comparative evaluation validates the tested piles' reliability against established standards and highlights the importance of selecting appropriate interpretation methods based on project-specific requirements and geotechnical considerations.

For Site B, the Static and Pile Dynamic Analysis testing yielded diverse capacities, indicating a high discrepancy when interpreted through various methodologies. The data, detailed in Table 4-5, distinguishes the Pile Dynamic Analysis (italicized entries) from the Static Load Tests (bold entries), presenting a complex picture of pile behavior under different testing conditions (Figure 4-29). The analysis reveals interesting trends in pile capacities and driving characteristics across the site. Piles B-1, B-2, B-3, and B-4 consistently demonstrate higher PDA capacities than the Static Load Testing method. This disparity suggests that PDA is more sensitive to certain soil conditions or pile behavior, leading to a more nuanced assessment of pile capacities. The observed variations in the number of blows required for the final 1 meter of driving further elucidate the complexity of soil-pile interactions. Piles B-1, B-2, and B-4, with 317, 304, and 371 blows respectively, demonstrate a higher resistance during driving, possibly due to encountering denser soil layers. However, piles B-3, B-7, and B-9 needed 217, 295, and 265 blows, respectively, for the last 1m during driving, indicating less resistance.

The PDA tests, conducted shortly after pile installation, show variances in mobilized energy and settlements, while the Static Load Test results, which involve testing to failure, provide a definitive measure of pile capacity. Piles B-7 and B-9, with better match qualities, demonstrate a good correlation between capacities determined by PDA and Static Load Test methods.

These findings underscore the importance of considering soil heterogeneity and pile driving characteristics in pile capacity assessments. The higher capacities observed in PDA for certain piles may indicate a need for targeted site investigations or adjustments in design parameters to account for variations in soil properties. Additionally, the differences in driving resistance highlight the dynamic nature of soil behavior during pile installation, emphasizing the need for comprehensive testing methodologies that can effectively capture these nuances.

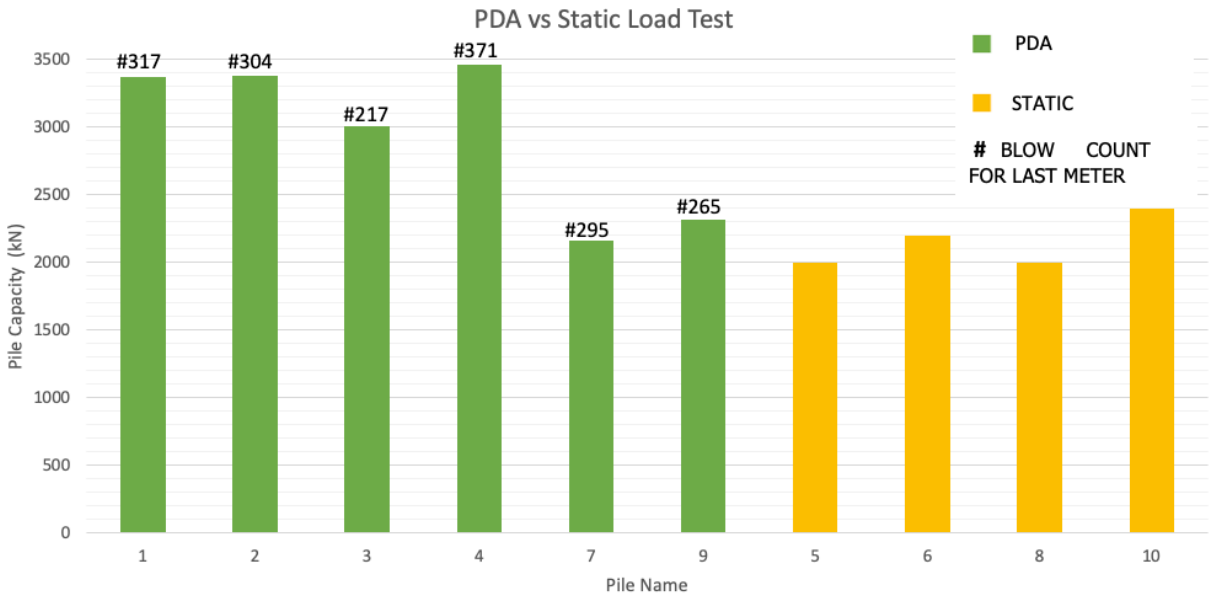

Figure 4-29 Capacity Comparison for Site B

Table 4-5 Pile Capacity Comparison for Site B

Pile_Name	Lenght (m)	Width (cm)	Ins_Date	PDA Date	Static Date	Ins vs Static (Days)	E_max (kNm)	Set (mm/bl)	Ru (kN)	Match Quality	Bearing Stratum
B-1_RD	16	40	7/30/15	RD_20mins			56	4.00	3370	3.57	Marl
B-2_RD			7/30/15	RD_20mins			53	4.80	3380	3.16	Marl
B-5			8/22/15		12/24/15	124.00			2000		Silty Sand
B-6			8/20/15		12/17/15	119.00			2200		Marl
B-3_RD			7/30/15	RD-20min			55	6.00	3004	2.64	
B-4_RD			7/30/15	RD-20min			47	2.00	3458	3.19	
B-7			6/15/17	8/4/17			37.4	6.00	2163	2.7	
B-8			6/15/17		9/25/17	102.00			2000		
B-9			10/7/15	11/9/15			54.7	9.50	2319	1.68	
B-10			7/1/17		8/21/17	51.00			2400		

In the Table 4-5, RD indicates the time of a Redrive, Ins_Date is the date on which the pile was instaled, PDA_Date and Static_Date are times on which tests were conducted, Ins vs Static measures the time difference between the pile installation and the subsequent Static Load Testing, E_max is the Maximum Energy delivered to the pile by the hammer during driving, Set quantifies the Settlement per blow, Ru captures the Ultimate Capacity of the Pile, and Match Quality is an assessment of the Quality of Signal Matching.

Furthermore, the static load test of B-11 (Figure 4-13), which did not progress to failure but instead was tested under a safety factor of two, exhibits an elastic behavior distinctly different from that of piles driven to failure. A comparative study of B-8 (Figure 4-13) and B-11 (Figure 4-11), positioned merely 20 meters apart, further illuminated disparities in behavior during the elastic portions of their respective static load tests. B-8 underwent a settlement of 21mm, whereas B-11 exhibited a significantly reduced settlement of only 7mm when subjected to the same load magnitude. This contrast points to a potential variance in local soil-structure interaction and stresses the inherent individuality of pile performance within similar geological settings. Such disparities in the behavior of piles situated in proximity reinforce the hypothesis that local variations in soil composition and properties can significantly influence the performance outcomes measured by both Static Load Testing and Pile Dynamic Analysis.

Further examination of the data reveals that the interpretation of Pile Dynamic Analysis results tends to be more comparable to static load test results when supported by higher-quality matches. This is exemplified by the cases of B-7 and B-9, where the agreement with static load test capacities was notably closer. These observations suggest that achieving and utilizing high-quality PDA data is essential for accurate capacity assessment, particularly in environments characterized by subsoil heterogeneity. Therefore, a comprehensive analysis approach, including both Static Load Test and PDA with careful consideration of match quality and soil consistency, is crucial for a nuanced understanding of pile capacity across varied geotechnical landscapes.

5. Conclusions and Recommendations

5.1 Conclusions

The comprehensive assessment of Pile Dynamic Analysis method and Static Load Testing across two sites in Kazakhstan provides significant insights into the capacity assessment of precast concrete piles. At Site A, the findings indicate a close correlation between the capacities determined by both PDA and Static Load Test when applied to the same piles bearing on cobble and gravel layers. Conversely, piles bearing on clay and silty-clayey sand layers show slight discrepancies. Site B exhibited notable discrepancies in the capacities assessed by the two methods, suggesting the influence of subsoil heterogeneity. Piles driven into the same stratigraphic layers (marl layer) show discrepancies in blow counts, ranging from 371 to 217 blows for the last meter of driving. By analyzing the data from both sites, the PDA method gives more reliable results in granular soils. For fine grained soils, the PDA method shows discrepancies. This may be related to the higher dynamic resistances of these soils, which is difficult to model in CAPWAP.

According to Nursultan, the construction manager in a local geotechnical company (personal communication, March 16, 2024), the cost-effectiveness and time efficiency of PDA compared to Static Load Tests are notable. PDA tests are five to ten times less expensive and faster, and they can be conducted up to ten tests in a single day, as opposed to the more extended period required for static aload testing.

Interpretation of Static Load Test result by Davisson's offset limit in North America differs from state to state. For example, Massachusetts Building Code Chapter 18 (2017) states that static load testing of piles should be interpreted as follows:

1) Theoretical Elastic Compression Line
2) Plus 0.15 inches (3.8cm)

3) Plus 1% of tip diameter or width in inches.

5.2 Recommendations

The study leads to the following recommendations for practice and further research:

1) Static Load Test and PDA Integration: According to the Kazakh Building Code (SNiP 5.01-01-2002), it is mandatory to conduct Static Load Testing on at least two or 1% of production piles or conduct PDA on at least six piles. Given the recent introduction of PDA in Kazakhstan, it is crucial to view PDA as a complement to Static Load Testing rather than a replacement. Higher safety factors should be applied to PDA results to account for the uncertainties associated with this new testing method. For instance, following the practice outlined by AASHTO section 10 (2010), where a safety factor of 2 is used for static load testing, a safety factor 2.5 should be applied for PDA results in Kazakhstan.
2) Energy and Settlement Control: Soil's dynamic resistance is generally considered a velocity-dependent resistance component (Rausch et al.2018). Therefore, contractors must meticulously select hammers to ensure sufficient energy transfer and that the pile's total static capacity is mobilized during testing. In cases where contractors lack hammers with sufficient energy capacity, applying a higher safety factor to PDA results becomes imperative to compensate for potential energy inadequacies.
3) Reliability of Signal Matching: The acceptability of a CAPWAP solution is not absolute and is generally determined by the Match Quality (MQ) value. Solutions with MQ above five are considered less reliable. However, this study found that some solutions with lower MQ values can yield significantly higher results compared to static load testing. Therefore, special attention should be given to match qualities, ensuring that the implications of

varying match qualities are thoroughly considered and addressed. Efforts should be directed towards improving the analysis, such as consulting independent experts to ensure data integrity and analysis reliability.

4) This study strongly recommends that the Kazakhstan government establish a centralized repository for geotechnical reports, PDA test results, and Static Load Test results, making them publicly accessible. Updating the current building code to mandate contractors to share these essential documents can incentivize the performance of high-quality pile tests and reliable reporting. Access to comprehensive data sets not only benefits future projects by providing valuable insights but also allows for the utilization of historical data in research and analysis, contributing to advancements in geotechnical engineering practices.

6. References

American Association of State Highway and Transportation Officials. (2010). LRFD bridge design specifications (5th ed.). Washington, D.C.

Aoki, N., & de Mello, V.F.B. (1992). Dynamic loading test curves. In F.B.J. Barends (Ed.), Application of Stress-Wave Theory to Piles (pp. 525-530). Rotterdam, the Netherlands: Balkema.

ASTM D1143. (1994). *Standard test methods for deep foundations under static axial compressive load*. ASTM International.

Augustensen, A. H., Andersen, L. V., & Sørensen, C. S. (2005). Time function for driven piles in clay. Department of Civil Engineering, Aalborg University, Aalborg, Denmark, Internal Report R0501.

Chen, C. S., Liew, S. S., & Tan, Y. C. (1999). Time effects on bearing capacity of driven piles. Proceedings of the 11th Asian Regional Conference, August 16-20, 1999, Seoul, South Korea.

Chow, F. C., Jardine, R. J., Brucy, F., & Nauroy, J. F. (1998). Effects of time on the capacity of pipe piles in dense marine sand. Journal of Geotechnical and Geoenvironmental Engineering, ASCE, 124(3), 254-264.

Davisson, M. T. (1972). High capacity piles. In *Proceedings, Lecture Series, Innovations in Foundation Construction* (pp. 81-112). ASCE, Illinois Section, Chicago, March 22.

Fellenius, B. H. (1980). The analysis of results from routine pile load tests. *Ground Engineering, 13*(6), 19-31.

Fellenius, B. H. (1984). Ignorance is bliss -- and that is why we sleep so well. *Geotechnical News, 2*(4), 14–15.

Fellenius, B. H. (1988). Variation of CAPWAP results as a function of the operator. In *Proceedings of the Third International Conference on the Application of Stress-Wave Theory to Piles* (pp. 814-825). Ottawa, May 25-27, 1988.

Fellenius, B. H. (2023). *Basics of foundation design* (Electronic ed.). Sidney, British Columbia, Canada.

Fellenius, B. H., Riker, R. E., O'Brien, A. J., & Tracy, G. R. (1989). Dynamic and static testing in soil exhibiting set-up. *Journal of Geotechnical Engineering*, 115(7), 984-1001.

Goble, G., & Hussein, M. (2000). Geotechnical special publication No. 94, Proceedings of sessions of ASCE specialty conference on performance confirmation of constructed geotechnical facilities (pp. 113-123). Amherst, MA.

Goble, G., Kovacs, W., & Rausche, F. (1972). Proceedings of the Specialty Conference on Performance of Earth and Earth-Supported Structures (pp. 3-38). American Society of Civil Engineers. Lafayette, IN.

Goble, G., Likins, G., & Rausche, F. (1975). *Bearing capacity of piles from dynamic measurements, final report*. Case Western Reserve University.

Goble, G.G. and Rausche, F., (1976), "Wave Equation Analysis of Pile Driving-WEAP Program." Volumes 1 through 4, FHWA #IP-76-14.1 through #IP-76-14.4.

GOST 10180. (2012). Methods for strength determination using reference specimens.

GOST 18105. (2018). Concretes. Rules for strength control and assessment.

GOST 19804-2012. (2012). Precast reinforced concrete piles.

GOST 8829. (2018). Precast reinforced concrete and concrete products. Load testing methods.

Hannigan, P., Ryberg, A., & Moghaddam, R. (2020). Identification and Quantification of Pile Relaxation.

Hussein, M., & Likins, G. (1993). Driving long precast concrete piles. In Proceedings of the 14th International Congress of the Precast Concrete Industry (p. 1). Washington, D.C.

Hussein, M., & Likins, G. (1993). Driving long precast concrete piles. In Proceedings of the 14th International Congress of the Precast Concrete Industry. Washington, D.C.

Institute of Geological Sciences of Kazakhstan. (n.d.). Engineering Geological Surveys for Construction [PDF]. Retrieved from https://igis.kz/images/snip/ntd-geolog-izyskaniya/sp-rk-1-02-02-102-inzhenerno-geologicheskie-izyskaniya-dlya-stroitelstva.pdf

Komurka, V., Wagner, A., & Edil, T. (2003). A review of pile set-up. In *Proceedings of the 51st Annual Geotechnical Engineering Conference* (pp. 105-130). University of Minnesota, St. Paul, MN.

Lee, W., Kim, D., Salgado, R., & Zaheer, M. (2010). Setup of driven piles in layered soil. Soils and Foundations, 50(5), 585–598. https://doi.org/10.3208/sandf.50.585

Likins, G. E., Fellenius, B. H., & Holtz, R. D. (2011). Pile driving formulas—Past and present. In M. H. Hussein, R. D. Holtz, K. R. Massarsch, & G. E. Likins (Eds.), *Geotechnical Special Publication 227: Full-scale Testing in Foundation Design* (pp. 737-753).

Likins, G., & Rausche, F. (2004). Correlation of CAPWAP with Static Load Tests. *Proceedings of the 7th International Conference on the Application of Stresswave Theory to Piles*, 153-165. Petaling Jaya, Selangor, Malaysia.

Likins, G., & Rausche, F. (2004). *In Proceedings of the Seventh International Conference on the Application of Stresswave Theory to Piles* (pp. 153-165). Selangor, Malaysia.

Lukpanov, R. E. (2016). Comparison of results of series pile load test in accordance with ASTM and Kazakhstan standards. Japanese Geotechnical Society Special Publication, 2(37), 1323-1326. https://doi.org/10.3208/jgssp.KAZ-05

Lukpanov, R.E. Comparison of GOST and ASTM as to Soil Testing by Vertically Loaded Piles.Soil Mech Found Eng 52, 33–37 (2015). https://doi.org/10.1007/s11204-015-9303-2

Luo, W., Sandanayake, M., & Zhang, K. (2019, February 1). Direct and indirect carbon emissions in foundation construction – Two case studies of driven precast and cast-in-situ piles. *Journal of Cleaner Production*, p. 211, 1517–1526. https://doi.org/10.1016/j.jclepro.2018.11.244

Massachusetts Government. (2017). 780 CMR Ninth Edition, Chapter 18: Soils and Foundation Amendments [Website]. Retrieved from URL https://www.mass.gov/doc/780-cmr-ninth-edition-chapter-18-soils-and-foundation-amendments-0

Ministry of National Economy of the Republic of Kazakhstan. (2002). Foundations of buildings and structures (SNiP RK 5.01-01-2002). [CONSTRUCTION NORMS AND RULES].

Ministry of National Economy of the Republic of Kazakhstan. (2002). Pile foundation (SNiP RK 5.01-03-2002). [CONSTRUCTION NORMS AND RULES].

Oil & Gas Journal. (2013). Kashagan Oil Field Starts Production. [https://www-ogjcom.ezproxy.library.tufts.edu/drilling-production/productionoperations/article/17258297/kashagan-oil-field-starts-production].

Oil & Gas Journal. (2019). Chevron Hikes Tengiz Project Cost to $45.2 Billion. [https://wwwogj-com.ezproxy.library.tufts.edu/general-interest/article/14072337/chevron-hikes-tengizproject-cost-to-452-billion].

Paikowsky, S. G. (2006). *Innovative load testing systems* (NCHRP Web-Only Document 84, Project 21-08: Contractor's Final Report). National Cooperative Highway Research Program.

Paikowsky, S. G., Regan, J. E., & McDonnell, J. J. (1994). A simplified field method for capacity evaluation of driven piles (Report No. FHWA-RD-94-042). Federal Highway Administration, Turner-Fairbank Highway Research Center.

Pile Dynamics, Inc. (n.d.). PDA Proficiency Test Worldwide. Retrieved from https://pdaproficiencytest.pile.com/worldwide/?&country=64

Salnikov, V., Talanov, Y., Polyakova, S., Assylbekova, A., Kauazov, A., Bultekov, N.,

Musralinova, G., Kissebayev, D., & Beldeubayev, Y. (2023). An assessment of the present trends in temperature and precipitation extremes in Kazakhstan. Climate, 11(2),33.https://doi.org/10.3390/cli11020033

Samson, L., & Authier, J. (1986). Changes in pile capacity with time: case histories. Canadian Geotechnical Journal, 23(1), 174-180.

Schmertmann, J. H. (1991). The mechanical aging of soils. Journal of Geotechnical Engineering, ASCE, 117(9), 1288-1330.

Seidmarova, T. J. (2009). Assessment of the bearing capacity of driven piles based on static and dynamic load tests. (Doctoral dissertation). Astana, Kazakhstan.

Sellountou, E., & Roberts, T. (2007). The cost-effectiveness of dynamic pile installation monitoring: A case study (pp. 1–12). https://doi.org/10.1061/40940(307)7.

Svinkin, M. R. (2004). Some Uncertainties in High-Strain Dynamic Pile Testing. In *Geotechnical Engineering for Transportation Projects* (pp. 705-714). https://doi.org/10.1061/40744(154)57

Svinkin, M.R. (2002). Engineering judgement in determination of pile capacity by dynamic methods. In M.W. O'Neill & F.C. Townsend (Eds.), Deep Foundations 2002: An International Perspective on Theory, Design, Construction, and Performance (GSP 116, pp. 898-914). Reston, VA, USA: American Society of Civil Engineers.

Tang, L., Cui, Y., Chen, J., Yang, G., Sun, S., Li, G., Sun, Q., & Jia, H. (2023). Analysis and research on the difference of design codes for vertical bearing capacity of pile foundation in cold regions. Cold Regions Science and Technology, 206, 103723. https://doi.org/10.1016/j.coldregions.2022.103723

Thompson, W. R., III, Held, L., & Saye, S. (2009). Test pile program to determine axial capacity and pile setup for the Biloxi Bay Bridge. DFI Journal - The Journal of the Deep Foundations Institute, 3(1). https://doi.org/10.1179/dfi.2009.002

Tomlinson, M., & Woodward, J. (2008). *Pile design and construction practice* (5th ed.). Taylor & Francis.

Tulebekova, A. S. (2015). Control equipment for pile test according to American and Kazakhstan standards. *Modern Applied Science, 9*(6), 192. http://dx.doi.org/10.5539/mas.v9n6p192

Tulebekova, A., Zhussupbekov, A., Mussabayev, T., & Mussina, S. (2019). Geotechnical issues of testing piles on construction site of Astana. In Proceedings of the 2nd GeoMEast International Congress and Exhibition on Sustainable Civil Infrastructures, Egypt 2018 – The Official International Congress of the Soil-Structure Interaction Group in Egypt (SSIGE). https://doi.org/10.1007/978-3-030-01902-0_11

Vesic, A. S. (1977). Design of pile foundations. Washington, D.C.

Whitaker, T., & Cooke, R. W. (1961). A new approach to pile testing. In *Proceedings of the Fifth International Conference on Soil Mechanics and Foundation Engineering*. Paris.

Yenikeyeff, S. M. (2008). Kazakhstan's gas: Export markets and export routes. Oxford Institute for Energy Studies.

York, D. L., Brusey, W. G., Clemente, F. M., & Law, S. K. (1994). Set-up and relaxation in glacial sand. Journal of Geotechnical Engineering, ASCE, 120(9), 1498–1513.

Zhussupbekov, A., et al. (2018). Application of static compression load test of joint piles in seaport "Prorva" in the Caspian Sea coastal area (Western Kazakhstan). In *Proceedings of the First International Conference on Press-in Engineering 2018* (p. 83). Kochi.